QA:QA

Characterization of Colloids Generated from Commercial Spent Nuclear Fuel Corrosion

Activity Title: Testing/Colloid Report

Activity Number: PAWTP30A

November 18, 2002

Revised March 28, 2003

C. J. Mertz, Robert J. Finch, Jeff A. Fortner, James L. Jerden, Jr., Yifen Tsai, James C. Cunnane, Patricia A. Finn

Chemical Engineering Division
Argonne National Laboratory
9700 South Cass Avenue
Argonne, IL 60439

TABLE OF CONTENTS

LIST OF TABLES

LIST OF TABLES – contd.

LIST OF FIGURES

LIST OF FIGURES – contd.

ACRONYMS

ANL	Argonne National Laboratory
ATM	Approved testing material
BWR	Boiling water reactor
Conc	Concentration
CSNF	Commercial spent nuclear fuel
DHLW	Defense high level waste
DLS	Dynamic light scattering
EDS	Energy dispersive X-ray fluorescence spectroscopy
EELS	Electron energy loss spectroscopy
EJ-13	Groundwater from the U.S. Geological Survey well "J-13" near Yucca Mountain, Nevada, that has been modified by reacting it with crushed Topopah Springs tuff at 90°C for 80 days (composition given in Table 2)
ELS	Electrophoretic light scattering
HA	Humid air test (commonly referred to "vapor test" in previous reports)
HDR	High drip-rate test: nominal injection rate of 0.75 mL each 3 to 4 days (1.5 mL/week)
ID	Sample identification
ICPMS	Inductively coupled plasma mass spectrometry
J-13	Groundwater from the U.S. Geological Survey well "J-13" near Yucca Mountain, Nevada
LDR	Low drip-rate test: nominal injection rate of 0.075 mL each 3 to 4 days (0.15 mL/week)
PS	Polystyrene
PWR	Pressurized water reactor
SN	Scientific notebook
TEM	Transmission Electron Microscopy
UFL	(also, UF) Unfiltered leachate
YMP	Yucca Mountain Site Characterization Project
ZP	Zeta Potential

GLOSSARY OF TERMS

Acid-strip: A process during which the internal surface of a stainless-steel reaction vessel is soaked in an aqueous solution of nitric and hydrofluoric acids, in an effort to dissolve radionuclides that have adhered to the vessel's interior surface.

Colloid: (also, Colloidal Particles) Submicrometer-sized particles with at least one dimension between 1 and 1000 nm whose properties are governed by Brownian motion. Practical definition for colloids in this report is material collected from leachate that is passed through filters with pore sizes based upon available filter sizes (between 1 or 5 nm and 450 or 1000 nm).

Corrosion Products: Solid compounds that form on the fuel during corrosion.

Dissolved Species: (also, Dissolved Fraction) Subnanometer species (i.e., ions, etc) typically < 1 nm in size. Practical definition is limited to the smallest filter size available in these experiments (i.e., 2 or 5 nm).

EJ-13 water: Groundwater pumped from the U.S. Geological Survey well "J-13" in Nevada that has been reacted with crushed tuff at 90°C for 80 days.

Fuel: Multi-grain fragments of the approved LWR test materials, ATM-103, ATM-106, ATM-109A, ATM-109B, and ATM-109C.

Fuel matrix: The solid UO_2 and substituents that are contained in the structure of the UO_2 as a solid solution, and which comprises the majority of spent fuel. The fuel matrix is distinguished from material that has phase-separated from the original UO2 during or subsequent to burn up in the nuclear reactor.

Gold Retainer: A thin gold mesh perforated with ~200-μm holes that was placed at the base of the Zircaloy-4 holder in the ATM-103 and ATM-106 high-drip tests after the 7.3 yr test interval.

J-13 water: Groundwater pumped from the U.S. Geological Survey well "J-13" in Nevada.

Leachate: Water that has accumulated in the bottom of a test vessel at the end of a test interval.

Particulate: Material in leachate that is greater than 450 or 1000 nm (limited by largest filter employed for tests).

pH: The negative of the base-ten log of the hydrogen-ion concentration measured in the leachate, measured at ambient hot-cell temperature (~25 – 30°C).

Sequential Filtration: A process whereby an aliquot of leachate is passed, through a series of filters with incrementally decreasing pore sizes. The series of filters consist of, first, a filter with 1000-nm pores, followed by a filter with 100-nm pores, and, finally, a filter with 50-nm pores.

Speciation: Classification of species or components based upon size (i.e., dissolved, colloidal, and particulate).

Unsaturated Tests: Tests under oxidizing conditions in which the relative humidity is 100%. There are three test types. They include a vapor test in which water vapor is present, a low-drip test in which a small amount of a simulated groundwater, EJ-13, is injected, and a high-drip test

in which ten times the amount of a simulated groundwater, EJ-13, is injected as in the low-drip test.

Zircaloy Holder: A cylindrical metal cup, 1 cm diameter x 1.5 cm tall, fabricated from Zircaloy-4 and used to hold the fuel fragments. The base of the cup contains 10-μm holes to allow solution drainage.

I. BACKGROUND AND SCOPE

A. Objectives

The purpose of this document is to summarize results on colloids generated from corrosion tests on commercial spent nuclear fuel (CSNF). Analyses presented here update results from on-going corrosion tests under Yucca Mountain repository relevant conditions (unsaturated testing at high drip rate, low drip rate and humid air conditions). In addition, the results from analyses on colloidal suspensions of uranium minerals phases in groundwater from Yucca Mountain or uranium saturated solutions are summarized.

B. Background

Colloids generated during waste form corrosion are potentially important in the performance assessment of the waste form in the repository. Colloids may transport radionuclides from a waste storage or disposal site in excess of amounts predicted solely on radionuclide elemental solubility limits. Recent studies at the Nevada Test Site (an unsaturated environment similar to Yucca Mountain) have shown the mobility of plutonium to be associated with colloids composed of clays, zeolites, and cristobalite [Kersting]. Numerous studies on nuclear waste glass corrosion have shown that clay colloids form and are prevalent in solution [Ebert; Buck; Geckeis]. However, few colloids have been detected in corrosion tests with commercial spent nuclear fuel [Finn 1994]. Likewise, colloidal transport has not been found to be a major mechanism for the transport of uranium at many natural analogue sites [Short; Miekeley]. However, experimental work on the formation of uranium oxide sols at pH and temperatures likely for a repository suggest that uranium substrate colloids must be considered [Ho].

The stability of dispersed colloids is dependent on numerous variables including pH, temperature, solution composition, etc. Colloidal interactions represent a balance between their dispersive properties (chargee repulsion) and their tendency to aggregate or sorb (intermolecular attraction). The ability to determine characteristic features of dispersed particles, such as size, shape, and surface potential, is important in determining their stability and behavior (i.e., dispersion, aggregation, or sorption) under a range of relevant environmental conditions. As such, this report presents results on the characterization of the physical and chemical nature of the solution-borne colloids that form during degradation of the waste forms, specifically as related to actinide releases.

This report summarizes the results of analyses on colloids from unsaturated corrosion tests on commercial spent nuclear fuel (CSNF) completed to date (8.7 years of testing for the CSNF) and not included in previous data reports. On-going unsaturated corrosion tests on CSNF were sampled periodically during the corrosion testing and the test solutions were analyzed for colloids to determine the nature of the colloids. The CSNF corrosion tests consist of two pressurized water reactor (PWR) fuels (ATM-103 and ATM-106) and three boiling water reactor (BWR) fuels (ATM109A, ATM109B, and ATM109C) being tested under unsaturated conditions at 90°C. These tests combine periodic injection of tuff-equilibrated J-13 groundwater into a sealed, stainless steel vessel containing fuel fragments in a zircaloy-4 sample holder at 90 °C. In

addition, colloidal suspensions of meta-schoepite and UO_{2+x} under saturated test conditions (in 10 mM uranyl nitrate or J-13 groundwater) at room temperature were characterized and are summarized in this report.

C. Previous Data Reports

The unsaturated tests with the ATM-103 and ATM-106 fuels were begun in September 1992 and, except for a six-month interruption during the first half of 1998, have been operating continuously during the 10 years since test initiation. Data obtained from these tests prior to 5.2 years have been reported previously (CRWMS M&O 2000) and will not be reported here. Data reported here correspond to samples taken during test intervals 5.2 through 8.7 years of reaction. Unsaturated tests with the ATM-109 fuels were begun in 1998 and have been operating continuously for over three years. Data reported for the ATM-109 fuel tests correspond to test intervals from test initiation through 3 years of reaction.

The unsaturated tests were run at 90°C and cooled to ambient temperature at test sampling. During the test interval, the leachate dripped from the fuel in the holder into water at the base of the vessel solutions (a Type 304L stainless-steel vessel). At the test sampling, the vessel was cooled to ambient laboratory temperature over a relatively brief period (typically less than 30 minutes). The concentrations reported in this report are those measured in aqueous solutions recovered from test vessels and measured at ambient temperature. Radionuclide "concentrations" reported in the previous data report for these tests (CRWMS M&O 2000) were not measured, but were calculated by determining the total mass of a given radionuclide recovered from each test vessel, including the mass in leachates plus the mass recovered during acid-stripping of reaction vessels, and dividing that total mass by the volume of solution recovered from each vessel during each sampling interval. Reporting such calculated concentrations was rationalized by the presumption that the total mass of every radionuclide recovered from each reaction vessel had been in solution at 90°C (as dissolved ions, colloids and/or particulates) when leachate dripped from the holder into water at the base of a vessel prior to sampling the leachate at ambient laboratory temperature. It would be difficult to determine the accuracy of this assumption due to the test configuration. Primarily for this reason, concentrations reported in this data report are those directly measured in the leachate at ambient temperatures and are, therefore, free of assumptions about what the concentrations of any radionuclide might have been at any temperature besides ambient (~25°C). The masses of nuclides removed from the vessel walls by acid stripping are also reported elsewhere (Finch et al. 2002).

In the previous report (CRWMS M&O 2000), Pu concentrations associated with colloids were determined from alpha spectrometry measurements of filters (50, 100, 1000 nm pore sizes) or the filtrate from a 5 nm pore size filter. The alpha spectra for the filters and filtrates (alpha planchets prepared by evaporation for the filtrates) typically have poor peak shape due to inelastic scattering from evaporites or alpha particles embedded in the membrane filter. Ideally, the alpha source should be a monolayer of alpha emitters which is achieved by electrodeposition (Schultz). This report uses alpha spectrometry measurements for Pu from filtrates that were electroplated or ICPMS results from filtrates for U or Pu isotopes. Dissolution of the filters followed by electrodeposition of the alpha emitters was not pursued.

D. Test Planning and Related Documentation

The principal investigator for this task is Carol Mertz. The test plan covering colloid work is "Waste Form Colloids Characterization and Concentration Studies" (SITP-02-WF-003, Rev. 00). The experimental work was performed in accordance with the Bechtel SAIC Company (BSC) prepared "ANL Statement of Quality Assurance Requirements," as implemented through the "Quality Assurance Plan for Technical Activities in Support of the Yucca Mountain Program" (YMP-02-001) and the associated Implementing, Administrative and Operating Procedures.

The work in the test plan is done in support of the License Application for the Yucca Mountain Project (YMP) as administered by Bechtel SAIC Company, LLC. This test plan was developed under the "Technical Work Plan for Waste Form Degradation Testing and Analyses in Support of SR and LA," TWP-WIS-MD-000008, Rev. 02.

This work supports the Total System Performance Assessment for the License Application (TSPA-LA) for a repository at Yucca Mountain, Nevada. More specifically, data obtained from this Task are to be used in the LA updates of the product document: MDL-EBS-PA-000004, Rev. 00. The documents supported by this test plan are covered by the technical work plan (TWP-WIS-MD-000008, Rev. 02).

E. Scope of Data Package

Data contained in this data package include concentrations measured in leachates and filtrates recovered from eleven corrosion tests conducted on three types of commercial spent UO_2 fuels (ATM-103, ATM-106, ATM-109). Three ATM-109 fuels were tested: ATM-109A, ATM-109B, and ATM-109C (a Gd-doped fuel). Test conditions include exposure of the fuels to modified groundwater ("EJ-13") at two rates of injection, as well as exposure to air saturated with water vapor (100% relative humidity). Descriptions of the test configurations and test matrices are given briefly in the following sections (additional information can be obtained in Finch et al. 2002).

The period covered by this report is for testing and sampling intervals following 5.2 years of reaction. The unsaturated fuel-corrosion tests at ANL were started in mid 1992 and the sampling intervals up to and including 4.8 years of reaction (i.e., data collected through mid 1997) were reported in a previous data package (CRWMS M&O 2000). The data reported here correspond to those collected from late 1997 through the end of 2001.

II. DATA ACQUISTION AND ANALYSIS

A. Experimental and Analytical Details

1. Experimental design

Two pressurized water reactor (PWR) fuels and three boiling water reactor (BWR) fuel types were used in the ANL corrosion tests. Testing on the corrosion of PWR and BWR fuels has been conducted for over eight and three years, respectively. The PWR fuels are designated ATM-103 and ATM-106. The ATM-103 fuel has a nominal burnup of 30 (MWd)/kg-U and a fission-gas-release of 0.25% (Guenther et al. 1988a). The ATM-106 fuel has a nominal burnup of 43 (MWd)/kg-U and a fission-gas-release of 11% (Guenther et al. 1988b). The BWR fuels are designated ATM-109A, ATM-109B, and ATM-109C. The three ATM-109 fuels came from three different fuel rods and have a range of burn-ups 64 to 72 (MWd)/kg-U. The ATM-109C fuel is doped with 2% Gd (Wolf et al., 2000).

For the ATM-103 and ATM-106 fuel tests up to the 6.8 year sampling, the fuel fragments were contained in a Zircaloy-4 holder that had a Zircaloy-4 retainer with 10-μm-diameter holes at its base. The small hole size at the base of the holder precluded fuel grains larger than 10 μm-diameter from being entrained with the leachate. The Zircaloy-4 retainers in the high-drip tests on ATM-103 and ATM-106 were replaced with new Zircaloy-4 retainers (with 10-μm-diameter holes) at the end of the 6.8-yr sampling interval; and these were subsequently replaced by gold retainers with 200-µm-diameter mesh size at the end of the 7.3-yr sampling interval. The Zircaloy-4 holders are housed in Type 304L stainless steel vessels. At the start of each test interval, the test vessel base contains approximately 5 mL of EJ-13 for drip tests and approximately 10 mL for vapor tests to ensure 100% relative humidity. The Zircaloy-4 holder is set on a ledge inside the test vessel. The vessel is sealed with a copper gasket and placed in a 90°C oven. For the drip tests, the top of the vessel is connected to a water injection system. Every 3 to 4 days, EJ-13 is injected onto the fuel in the high-drip and low-drip tests and air is flushed into the vessel to replenish the air. The injected water is determined by the increase in mass at the end of a test interval. In addition, the mass of water delivered with ten injections is measured at each test interval to determine the change in the injection system due to wear and radiation damage. The oven temperature is monitored and recorded with a data-logger, which records the temperature twice per 24-hr period and alarms for deviations greater than ±2°C. Further details on the test descriptions is provided in (CRWMS M&O 2000), (Finn et al. 1994), and (Finch et al. 2002).

Characteristics of the fuels used in these tests are summarized in Table 1.

Table 1. Characteristics of CSNF Fuels used in Unsaturated Drip Tests

Fuel	ATM-103	ATM-106 (NBD107)	ATM-109A (QCF1)	ATM-109B (QC B1A)	ATM-109C (QC D4A)
Reactor type	PWR	PWR	BWR	BWR	BWR
Nominal Burn-up (MWd/kg-U)	30[a]	43[b]	71[c]	72[c]	64[c]
Fission Gas Release (%)	< 0.25[a]	11[b]	4.4[c]	2.95[c]	3.5[c]
Years out of reactor at test initiation	12[a]	12[b]	7[c]	7[c]	7[c]
Test Type [d]	HDR LDR HA	HDR LDR HA	HDR HA	HA	HDR HA
Test Initiation	1992	1992	1998	1998	1998
Total Reaction Time	>10 yr	>10 yr	4 yr	4 yr	4.yr

[a] Guenther et al. (1988a) PNL-5109-103.
[b] Guenther et al. (1988b) PNL-5109-106.
[c] Wolf et al. (1999) YMP Data Report (YMP/SF-3A-319).
[d] HA = humid-air tests (also known as vapor tests), LDR = low drip-rate tests, and HDR = high drip-rate tests

2. Analytical methods

The characterization and quantification of colloids generated in the corrosion of CSNF under Yucca Mountain repository-relevant test conditions is essential to determine important waste form colloidal parameters that are necessary for predicting the radionuclide-associated colloid concentrations. The sampling of the tests and the various characterization techniques employed to characterize and quantify the colloids will be discussed in the following section.

CSNF Test Sampling Procedure

Each test was sampled periodically. During each sampling interval, the tests were interrupted to remove leachate and solid samples. Each test vessel was removed from the 90°C oven and cooled by placing the base of the vessel in contact with dry ice. Once cooled, the vessel was opened and the Zircaloy-4 holder with the reacted fuel fragments was removed and examined under an optical microscope.

Leachate was removed from the used test vessel and divided into aliquots (if a sufficient volume of leachate is available) for analysis by inductively coupled plasma mass spectroscopy (ICPMS), high-resolution alpha spectrometry, gamma spectroscopy, and dynamic light scattering. Alpha spectroscopy was discontinued after 2000; after the 7.7 and 1.5 year samplings

for the ATM-103 or ATM-106 and for the ATM-109 fuels, respectively. Selected aliquots were filtered as described below and the filtrates were also analyzed by ICP-MS, gamma spectrometry and alpha spectrometry, depending on the volume of liquid available. The pH of the leachate was measured at room temperature. After removing leachate from the test vessel, the interior of the test vessel was filled with an acid solution overnight at 90°C in order to dissolve any material remaining in the vessel.

Filtration

Filtration was used to separate various sized species (i.e., dissolved, colloidal, micron-sized particulate). The elemental composition and activity of radionuclides associated with each size fraction were determined using inductively coupled plasma-mass spectrometry and/or by nuclear spectroscopy (alpha and gamma spectrometry), respectively. Alpha spectrometry data are not available for sampling periods after January 2001. Several types of filters were employed for filtering the test solutions (cone, membrane, and microcentrifuge filters). Typically, an aliquot of all test solutions was passed through a 5 nm cone filter (the smallest pore size employed to determine the dissolved concentration; practical definition for dissolved species based upon available filters) and then centrifuged to recover the filtrate. In addition, sequential filtration of the test solution through a series of membrane filters with decreasing pore sizes was performed, if sufficient solution was available. The membrane filters were assembled in filter housings and the solution was passed through the membrane filter unit using a syringe. Additional filters were employed in 2000 for filtration of the test solutions. These filters were microcentrifuge filters of the following sizes: 200 and 450 nm. An ultracentrifuge was used to recover the filtrates for analysis.

Inductively coupled plasma mass spectrometry (ICPMS)

ICPMS is used to quantitatively analyze for most radionuclides; of interest here are mass numbers of uranium and the transuranium actinides, Np, Pu, Am, and Cm. Actinides analyzed by ICPMS include four isotopes of uranium: U-234, U-235, U-236, U-238; one neptunium isotope: Np-237; three plutonium isotopes: Pu-239, Pu-240, Pu-242; two americium isotopes: Am-241, Am-243; and Cm-244. Several of these isotopes can also be measured by other methods (see below). Results presented in this report include isotopes of uranium and Pu-239.

Potential isobaric interferences that can affect the accuracy and precision of ICPMS analyses of concern here include several natural isotopes present in EJ-13 water, notably the three most abundant isotopes of uranium (234, 235, and 238), as well as radiogenic isotopes from the fuel. This interference is expected to be relatively small for U-238 and Pu-239.

High resolution alpha spectrometry

High-resolution alpha spectrometry provides quantities of the following alpha-emitting isotopes: Pu-239 + Pu-240, Cm-244, Am-241 + Pu-238, Np-237, and Am-243. Alpha spectrometry cannot distinguish between the two Pu isotopes, Pu-239 and Pu-240; nor can Am-241 be distinguished from Pu-238. Calculating individual contributions from these two pairs of isotopes to alpha spectra requires knowledge of the relative contributions of each. It is reasonable to assume that Pu isotopes do not fractionate in these tests, and we can, therefore, use the ratio of Pu-239 to Pu-240 in the fuel being tested; these ratios are available from ORIGEN2 calculations tabulated by Guenther et al.(a and b) for ATM-103 and ATM-106. The

corresponding ratios for the ATM109 fuels are those determined by direct analysis of the fuel and reported by Wolf et al. (2000).

Americium and Pu might be expected to behave in chemically distinct ways, so that deconvoluting contributions to alpha spectra by Pu-238 and Am-241 is less straightforward. Because Pu-238 is expected to behave chemically the same as Pu-239 and Pu-240, the concentration of Pu-238 relative to the other Pu isotopes in a particular sample should be proportional to its relative concentration in the fuel. The corresponding concentration of Pu-238 might then be extracted from the combined contribution from both Am-241 and Pu-238 in the alpha spectrum using the concentration of Pu-239 and Pu-240 determined by alpha spectroscopy and subtracting the appropriate amount of Pu-238 from the combined Am-241+Pu-238 concentration measured by alpha spectrometry. In this way, confidence in the concentration of Pu-238 and, therefore, Am-241 determined by alpha depends on the analysis of Pu-239 and Pu-240 from the same sample. However, Am-241 is also analyzed by ICPMS and by gamma spectrometry, and Am-241 concentrations for a particular sampling interval can be compared among the three independent methods used, when available.

While both the ICP-MS and alpha techniques detect plutonium, the plutonium quantities are best quantified by alpha spectrometry where concentrations as low as 0.001 ppb are easily measured (at least an order of magnitude lower than detection limits obtained using ICP-MS). The americium is, in general, most accurately determined by the gamma spectroscopy, owing to its very low concentration in solution (americium is generally below detection limits for alpha spectrometry).

The alpha spectrometry samples were prepared by electroplating the solution and, at earlier sampling periods, were also prepared by evaporation. Electroplating the solution affords higher energy resolution than evaporation by reducing the inelastic scattering that plagues thick samples (electroplating minimizes salt evaporates). When combinations of evaporated and electroplated alpha spectra are available, data from electroplated samples were used in this report.

Gamma Spectroscopy

Gamma spectroscopy is used to quantify several radioisotopes, including Am-241, Cs-134, and Cs-137. Limited filtration data is available from gamma spectroscopy for Am associated with colloids, as such this data is not presented.

Dynamic Light Scattering (DLS)

Dynamic light scattering is used to determine the size of particles in the colloidal size range. Particle size calibration is performed using polystyrene (PS) size standards (nominal sizes of 30, 70, 100 and 300 nm). Conversion of the count rate to a number concentration for the uranium substrate colloidal suspensions in this study is based upon a calibration curve for polystyrene (PS) size standard solutions (Figure 1). Polystyrene solutions were diluted using ultrapure water (deionized, resistivity of 18 megaohm·cm) and the count rate was measured at a scattering angle of 90°. Colloid number concentrations for the uranium substrate suspensions were estimated assuming that the uranium substrate colloids are spherical and scatter light as efficiently

as the PS standards (the scattering intensity is proportional to the refractive index). Both of these assumptions are limited in their application for obtaining the absolute concentrations for the uranium substrate colloids, but are useful in examining trends. The refractive index of PS is 1.6 [Schurtenburger] compared with 2.4 for UO_2 [Ho]. Multiple DLS measurements were performed on each sample by varying experimental parameters. For stable colloidal suspensions, the size distributions were reproducible. Intensity weighted distributions are presented in this report.

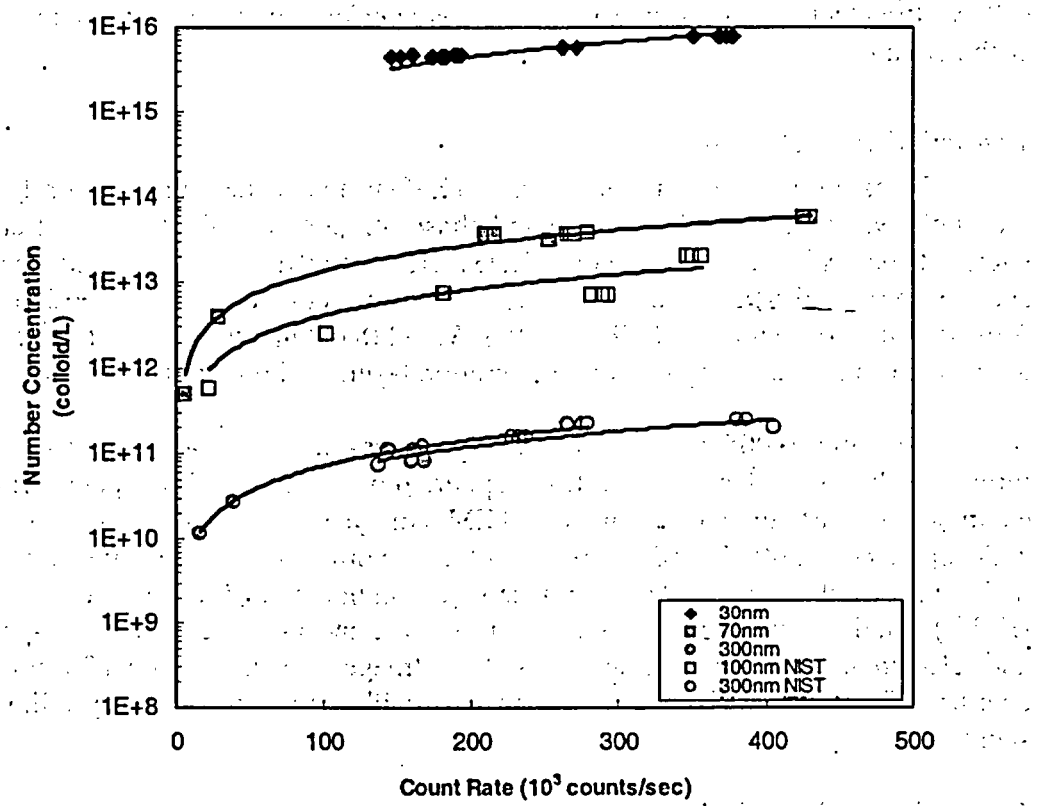

Figure 1. Relationship between measured count rate and calculated number concentration for polystyrene nanosphere size standards of nominal sizes.
Note: solid diamonds, 30 nm Duke Scientific Corp.; solid squares, 70 nm Duke Sci. Corp.; solid circles, 300 nm Duke Sci. Corp.; open squares, 100 nm NIST; open circles, 300 nm NIST). Solid lines represent linear least squares fit of data (equations for fits given in Table 2).

Table 2. Correlation between nanosphere size standards and DLS count rate.

Size/Manufacturer	Equation from Least Squares Fit of Data
30 nm Duke	Number Concentration (colloid/L) = 2e13 x Count Rate (kc/s)
70 nm Duke	Number Concentration (colloid/L) = 1e11 x Count Rate (kc/s)
100 nm NIST	Number Concentration (colloid/L) = 4e10 x Count Rate (kc/s)
300 nm Duke	Number Concentration (colloid/L) = 7e8 x Count Rate (kc/s)
300 nm NIST	Number Concentration (colloid/L) = 6e8 x Count Rate (kc/s)

Note: Equations used to convert count rate to number concentration for colloids of nominal size based upon least squares fit of data from nanosphere polystyrene size standards in Figure 1.

Zeta Potential Measurements

Zeta potential measurements were performed on a Zeta Plus unit from Brookhaven Instruments Corp. The performance of the instrument was checked with a mobility standard from NIST (geothite, SRM 1980). The measured mobility of the reference material was in excellent agreement with the certified mobility. The pH of the colloidal suspensions was adjusted to selected pH values with 0.1 M nitric acid or 0.1 M sodium hydroxide, and the solution was shaken to disperse the colloids prior to loading the sample in the electrophoresis cell. Multiple zeta potential measurements were performed at ambient laboratory temperature for each pH value.

Transmission Electron Microscopy

Transmission electron microscopy (TEM) is an excellent method for determining morphology, structure, and elemental and phase composition of colloid substrate materials [by energy dispersive x-ray spectroscopy (EDS), electron diffraction (ED), and electron energy loss spectroscopy (EELS)]. These techniques have been used to characterize colloid substrate phases formed in the corrosion of CSNF and DHLW and to obtain evidence that these colloid substrates are formed as a result of spallation of alteration layers and precipitated phases.

A small (~0.005 mL), unfiltered aliquot was collected from the test solution and wicked through a "holey" or lacey carbon film supported on a copper TEM support grid. The grid was examined for particulate material using TEM. Analyses were performed using a JEOL 2000FXII TEM operated at 200 kV and equipped with two Noran energy dispersive X-ray spectrometers, including a light element detector and also a Gatan 666 parallel electron energy loss spectrometer (EELS). Analysis of phases involved the use of the energy dispersive X-ray spectroscopy (EDS) and selected area electron diffraction (SAED). Images are taken using a 30-um objective aperture. The microscope camera lengths were calibrated using a polycrystalline aluminum standard.

Comparison of Isotopic Analyses

The two techniques used to analyze Pu-239 for this task (ICPMS, and alpha spectroscopy) have different sensitivities, detection limits, potential interferences, etc., so that masses and concentrations determined for Pu-239 by these analytical techniques may differ. Unless noted otherwise, there is no *a priori* reason to assign more or less confidence to any particular concentration value that has been analyzed by either of these analytical techniques. In fact, comparisons of concentrations for Pu-239 determined by these analytical techniques can provide useful information about analytical uncertainties. We have found that agreement within about 50% is common and reasonable with measured concentrations above approximately 0.1 ppb (Refer to Figure 2 for Pu-239 data analyzed by ICPMS and alpha spectrometry). As a rule, ICPMS is probably the least sensitive technique among those used here, and alpha spectroscopy the most sensitive (i.e., highest and lowest limits of detection, respectively). Isotope masses and concentrations that were analyzed but were below the lower limit of detection are indicated in the tables as "bd" (below detection). Entries in the tables that have a dash in place of an entry indicate isotope analyses that were not performed or are otherwise unavailable for any of several possible reasons, including a dry test vessel, insufficient solution volume, analytical problems, etc.

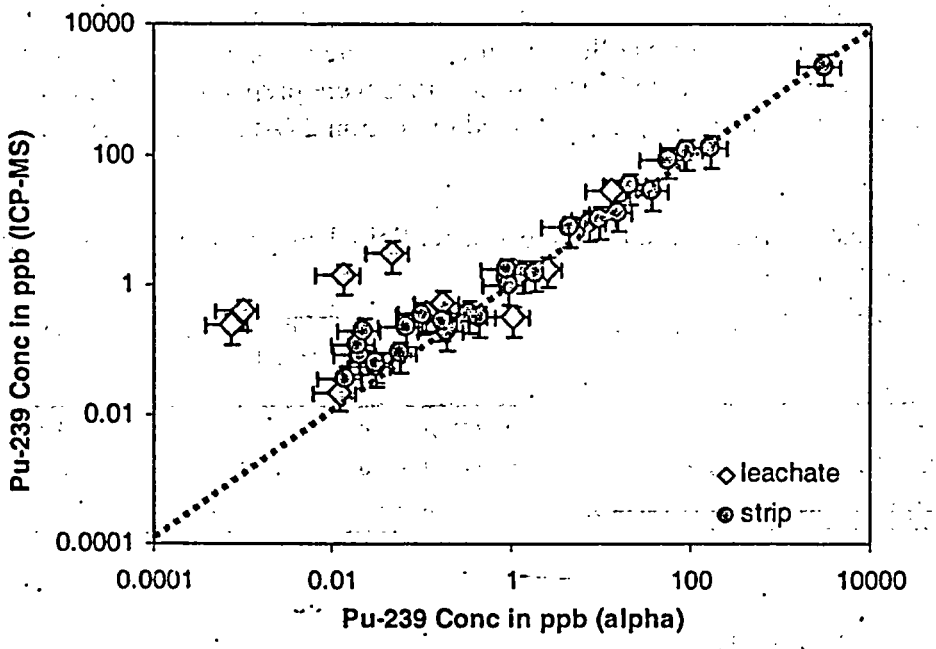

Figure 2. Comparison of Pu-239 concentrations analyzed by ICPMS and alpha spectrometry for leachate and strip solutions from CSNF corrosion tests.

Detection Limits

Mass releases and concentrations from intervals for which sample analyses were at or below the lower limit of detection for a given analytical method are not reported in the data tables. Isotopes present at concentrations at or below the lower limit of detection are reported as "less than" values to the task PI by the analyst. These detection limits vary among techniques and individual samples for a variety of reasons, some of which are generally applicable and others are unique to a particular sample or sampling interval; they are not reported here. Instead, all "less-than" values are reported here as "below detection" (designated as "bd" in the data tables).

B. Test Matrix

The test matrix for the CSNF tests is described in detail elsewhere (Finch et al. 2002). The unsaturated testing employs five fuels: ATM-103, ATM-106 and ATM-109A, ATM109B, and ATM-109C (refer to Table 1). The matrix includes six "drip" tests in which a modified groundwater, EJ-13, is injected periodically at two rates and five humid-air tests in which each test vessel is sealed with a small volume of water (~10 mL) but no water is injected between samplings. There are two (nominal) injection rates: 1.5 mL per week ("high") and 0.15 mL per week ("low"), with one-half the weekly injection volume being injected every three or four days. The tests are conducted at 90°C, which is in the range of expected repository temperatures approximately 1000 years after closure. One control test (injection vessel without fuel) is also being conducted, and samplings are performed for the control test in the same manner as for the other tests.

In addition, some test data are presented from hydrologically saturated tests with uranium dioxide and meta-schoepite colloids in uranyl nitrate or J-13 groundwater. The test matrix for these tests is shown in Table 3. The suspensions were prepared and the colloidal properties were characterized by the techniques described in Section 2 (Analytical Methods).

Table 3. Test matrix for uranium substrate colloidal suspensions in uranyl nitrate or J-13 groundwater.

Solution ID	Uranium substrate	Diluent	Conc of Uranium substrate in diluent (g/mL)	pH	Reference: SN/page
--	--	10mM uranyl nitrate	--	4.80	1831/10-11
CM1831/16-2	meta-schoepite and UO_{2+x}	10mM uranyl nitrate	0.0010	5.06	1831/16, 1830/35
CM1831/16-3	meta-schoepite and UO_{2+x}	J-13 groundwater	0.00019	7.66	1831/16, 1830/35

C. Data Analysis

All of the measured and derived variables presented in this report are summarized in Table 4. In the case of derived variables, the method of calculation is identified and the uncertainty estimates are given. The accuracy and precision, as well as experimental uncertainties, are discussed below.

III. DESCRIPTION OF THE DATA

A. Data Dictionary

Table 4 provides a data dictionary of the experimental and derived values for which data are included. Where appropriate, equations are presented to define derived variables. Values include the measured parameters (colloid size, zeta potential, actinide concentrations and activities) and the derived parameters (colloid concentrations).

Table 4. Summary of measured quantities, derived quantities and associated uncertainty estimates.

Value	Type[a]	Definition and Equation	Uncertainty
Solution mass	M	Mass (g) of solution sample aliquot (leachate or acid strip) determined gravimetrically (ICPMS, and alpha required different size aliquots)	0.005% ICPMS; 10% Alpha
ICPMS Nuclide Concentration (Conc.)	M	Concentration measured in leachate or acid strip sample by ICPMS.	±50%
Activity	M	Activity (Bq) measured in leachate or acid strip by alpha spectroscopy.	±50% Alpha
Alpha Nuclide Concentration (Conc.)	D	Concentration in leachate or filtrates; calculated from activity in aliquot. Conc (ng/g) = Activity (Bq) / Spec.Act.[b] (Bq/g) / Sol. Mass (g) * 10^9 ng/g	±50%
Mass Release derived from Alpha data	D	Mass (g) of nuclide released from sample to base of vessel (also used for acid strip mass release). Mass (g) in aliquot = Activity (Ci) / Spec.Act.[b] (Ci/g) Mass (g) in test = Mass (g) in aliquot / (test Vol. / aliquot Vol.)	±51%
Colloid Size	M	Colloid size (nm) measured in leachate by DLS.	±10%
Colloid Concentration	D	Colloid concentration determined from calibration curve with nanosphere standard solutions. Count rate (±30% based upon multiple DLS measurements) versus Mass (g) of nanosphere standard solution / standard Vol. (g)	±50%
Colloid Zeta Potential	M	Zeta potential of colloid measured in leachate by zeta potential measurements.	±15%

[a]Variable Types: D = derived; M = measured.
[b]Spec. Act. = specific activity in Ci/g or Bq/g.

Leachate Concentrations

Concentrations reported here were measured at ambient laboratory temperature (~25°C). Corrections of raw analytical data include a correction factor for dilutions of sample aliquots (where applicable), including addition of acid prior to analysis.

Seven categories of solution concentrations are reported: those corresponding to unfiltered leachates (UFL), and to solutions that were passed through filters of six nominal pore sizes, ranging from 1000 nm to 5 nm. Leachate concentrations from solutions that were filtered through 1000 nm, 100 nm and 50 nm filters were obtained by passing a single solution aliquot sequentially through filters with progressively smaller pore sizes, three filtration steps for each aliquot. Leachate concentrations from solutions filtered through 450 nm, 200 nm and 5 nm filters correspond to separate aliquots of unfiltered leachate, each aliquot being passed once through one filter in a single filtration step.

UFL (Unfiltered Leachate) as used in Appendix 2 is the mass in grams of a given analyte in the unfiltered leachate solution as measured at ambient laboratory temperature.

Leachate is the liquid water recovered from the base of each test vessel during a sampling interval. Selected aliquots of leachate are filtered by various means, as prescribed in the test-sampling procedure, and as volume allows. The volume of leachate for each sampling interval is determined calculated as the difference between the total mass of each test vessel at the start of the test interval and that at the end of the test interval. Leachate mass is converted to volume assuming the density of the leachate is 1 g/mL.

Filtrate is a leachate aliquot that was passed through a filter. Filtration data reported in the data tables correspond to leachate concentrations measured after passing aliquots of leachate through filters with pore sizes designated in the data tables; these concentrations were also measured at ambient room temperature.

The pH of all leachates was measured at ambient laboratory temperature.

B. Data Organization

Data are presented in Appendices 1 through 3 arranged primarily by fuel type (ATM-103, ATM-106, ATM-109) and test type (HDR, LDR, HA). Colloidal sizing data determined by DLS analyses are provided in Appendix 1 for all of the tests. Data tables showing leachate concentrations in parts per billion (milligram of each radionuclide per kilogram of solution) or *ppb* are already reported in (Finch et al. 2002). The concentration in ppb was converted to mol/L (refer to Table 5 for reference to the data tables in Finch et al. 2002). Concentrations of Pu-239 and U-238 (in molarity) determined by ICPMS and/ or alpha spectrometry analyses are provided in Appendix 2 for the high drip-rate tests (ATM-103 HDR, ATM-106 HDR, ATM-109A HDR, and ATM-109C HDR), the low drip-rate tests (ATM-103 LDR and ATM-106 LDR), and the humid-air tests (ATM-103 HA, ATM-106 HA, ATM-109A HA, ATM-109B HA, and ATM-109C HA).

Table 5. Summary of references to U-238 and Pu-239 concentration data.

Test ID	*Fuel*	*Test Type**	*Isotope*	*Data Table Reference Number* [a]	*Analysis Method* [b]
S31J	ATM-103	LDR	U-238	DTC-75	ICP
			Pu-239	DTC-80	ICP
			Pu-239	DTC-91	alpha
S61J	ATM-106	LDR	U-238	DTC-93	ICP
			Pu-239	DTC-98	ICP
			Pu-239	DTC-109	alpha
S32J	ATM-103	HDR	U-238	DTC-1	ICP
			Pu-239	DTC-6	ICP
			Pu-239	DTC-19	alpha
S62J	ATM-106	HDR	U-238	DTC-20	ICP
			Pu-239	DTC-25	ICP
			Pu-239	DTC-37	alpha
S3V	ATM-103	HA	U-238	DTC-109	ICP
			Pu-239	DTC-116	ICP
			Pu-239	DTC-127	alpha
S6V	ATM-106	HA	U-238	DTC-129	ICP
			Pu-239	DTC-134	ICP
			Pu-239	DTC-145	alpha
S9AJ	ATM-109A	HDR	U-238	DTC-39	ICP
			Pu-239	DTC-44	ICP
			Pu-239	DTC-55	alpha
S9CJ	ATM-109C	HDR	U-238	DTC-57	ICP
			Pu-239	DTC-62	ICP
			Pu-239	DTC-73	alpha
S9AV	ATM-109A	HA	U-238	DTC-147	ICP
			Pu-239	DTC-152	ICP
			Pu-239	DTC-163	alpha
S9BV	ATM-109B	HA	U-238	DTC-165	ICP
			Pu-239	DTC-170	ICP
			Pu-239	DTC-181	alpha
S9CV	ATM-109C	HA	U-238	DTC-183	ICP
			Pu-239	DTC-188	ICP
			Pu-239	DTC-199	alpha

* LDR = low drip rate; HDR = high drip rate; HA = saturated water vapor (humid air).
[a] Concentration data table number (Reference to tables in Appendix 2 of Finch et al. 2002).
[b] ICP = ICP-MS; alpha = alpha spectrometry
Note: The groundwater used in these tests is EJ-13 (refer to Finch et al. 2002 for details).

C. One-of-a-kind records

Supporting data are recorded in the scientific notebooks or are on file in the QA records at ANL.

D. Accuracy and Precision

Accuracy and precision of analytical measurements are estimated and discussed in this section. However, these measurement uncertainties do not include all components of experimental uncertainty. Factors such as differences in fuel segment inventories, pellet cracking patterns, or loss of fragments during test preparation or performance are not included in measurement uncertainties but are discussed below in the Uncertainties section.

Maximum estimates of measurement uncertainty were made for both ICPMS and gamma spectroscopy measurements based on replicate analyses of NIST-traceable standards analyzed according to approved standard operating procedures. For ICPMS, the maximum uncertainty is ±10% for elemental analyses and ±50% for nuclide analyses. Thus, the maximum measurement uncertainty is ±10% for reported elements such as potassium, calcium, and uranium, and ±50% for nuclides such as ^{90}Sr, ^{99}Tc, ^{129}I, ^{237}Np, and ^{239}Pu.

Solution volumes were determined by measuring the mass of an aliquot and dividing it by the density of the solution. All solution mass/volume determinations were made at ambient laboratory temperatures assuming that the density of the solutions was 1.0. The error associated with this assumption is around 0.2%. The weighed mass for aliquots for gamma and ICPMS analyses is typically 4 grams of solution with the balance accuracy being 0.0002 g. The relative magnitude of the error from this source is thus approximately 0.005% for each aliquot. The weighed mass for aliquots for alpha counting of the leachate, the 5-nm filtrate from the leachate, and the acid-strip is 0.20 g with the balance accuracy being 0.02 g. The magnitude of relative error from this source is thus approximately 10%.

The accumulation of indeterminate errors where the values with which the errors are associated are combined as sums or differences can be estimated by taking the square root of the sum of the squares of the individual absolute variances [Cunnane, 2001]. For example,

$$(S_y)^2 = (S_a)^2 + (S_b)^2 + (S_c)^2 + \ldots (S_n)^2 \qquad (1)$$

Where (S_y) is the standard deviation of the sum and (S_a), (S_b) and (S_c) are standard deviations of the values in the sum. The propagation of errors in the case of multiplication and division can be estimated in a similar way. For example,

$$(S_y)_r^2 = (S_a)_r^2 + (S_b)_r^2 + (S_c)_r^2 + \ldots (S_n)_r^2 \qquad (2)$$

Where in this case $(S_y)_r$ is the relative variance of the result of the multiplication or division calculation and $(S_a)_r$, $(S_b)_r$ and $(S_c)_r$ are the relative errors associated with the individual values in the calculation.

We can use this type of treatment to determine the dominant source of error in the data presented in this report. The values used in this estimate include errors associated with the density of water, the leachate mass determination, the aliquot mass determination and error associated with the analytical method.

Propagated Error for ICP-MS = $[(0.2)^2 + (0.005)^2 + (0.005)^2 + (50.0)^2]^{-0.5} = 50\%$

Propagated Error for Alpha data = $[(0.2)^2 + (0.005)^2 + (10.0)^2 + (50.0)^2]^{-0.5} = 51\%$

These error propagation estimates indicate that statistical errors in the analytical measurements dominate the uncertainties of these data. Similarly, it can be shown based on this methodology that the errors associated with derived quantities (e.g. see Table 4) that involve multiplications and divisions, such as nuclide fractional release values, will also be dominated by the errors associated with the analytical measurements (approximately ±50% for ICP-MS and alpha counting). Based on extensive characterization of ATM-103 and ATM-106 [Guenther, 1986 a,b], the uncertainty in the inventories is relatively small. ATM-109 has had significantly less characterization, but burnup analysis, gamma scan characterization, and inventory determination of selected nuclides was performed [Wolf et al., 2000]. A conservative value of ±10% is assigned to the estimate of uncertainty in fuel inventories. Thus, this source of uncertainty does not significantly increase overall uncertainties, as shown above, due to the relatively high errors associated with the analytical methods.

Uncertainties associated with these data and experiments include measurement uncertainties and uncontrolled experimental factors. Measurement uncertainties arise from determination of mass, calculation of volume, determination of particle sizes by filtration, and measurement of concentrations by ICPMS. Experimental uncertainties include localized inhomogeneity of nuclides in irradiated metallic uranium fuel, loss of sludge particles from the sample holder during sampling operations, and most significantly the extrapolation of results from only two samples of irradiated fuel.

Separation of nano-scale charged particles by means of filtration is subject to errors associated with charge interactions between particles and filter substrate and uncertainties associated with filtration of particles with irregular morphology. However, because excellent particle size agreement was observed for waste form colloids using three technically unrelated methods of colloid analysis (TEM, DLS, and filtration/ICP-MS), the uncertainty associated with colloid filtration is considered small. Together, these measurement errors are considered negligible relative to the maximum error associated with ICP-MS measurements which is ±50% for nuclides. Thus the measurement uncertainty for the values reported is estimated at ±50%.

E. Uncertainties

The primary sources of uncertainty, other than analytical accuracy and precision, associated with the unsaturated tests are: (1) those introduced by the original test design, (2) those introduced by reconfiguration of the experimental set-up, (3) those introduced from inevitable experimental problems, such as vessels going dry and small pieces of fuel falling into the leachate, and (4) those introduced by the uncontrolled experimental factors that may influence the dissolution behavior (nuclide release) of the spent fuel samples.

Some uncertainty about the nature of the colloids generated in the unsaturated tests is derived from the original experimental set-up due to a number of factors: the influence of pH and temperature, the flow of the groundwater over the fuel, the influence of the fuel holder's hole size at the base, and the sorption behavior in the leachate reservoir (or test vessel). These tests were designed to simulate CSNF degradation under a likely water contact scenario at YM, however, in terms of individual processes that occur, the data they yield is often difficult to interpret. One must attempt to deconvolute the various processes (sorption, diffusion, sedimentation, etc) effecting various experimental parameters of interest (i.e., the concentration of colloids generated during corrosion of CSNF).

First, the stability of colloids is known to be influenced by pH (which is dependent upon colloid phase composition and surface charge characteristics), thus the transport of any colloids from the local conditions at the fuel and holder to the solution in the vessel would most likely result in a large pH and solution chemistry difference. The solution in the bottom of the collection vessel most likely evolves during the test duration, but it will probably never represent the local pH at the surface of the fuel and alteration products. As such, large differences in the solution chemistries may promote lower concentrations of colloids through destabilization, deposition or sorption mechanisms.

The transport of colloids in an unsaturated environment is influenced by the film thickness of the groundwater [Wan and Wilson]. Wan and other researchers [Wan and Wilson, Wan and Tokunaga, Veerapaneni et al. 2000, Lenhart and Saiers] have shown that a critical thin film thickness for a given particle size exists which inhibits colloid transport. The film thickness in the CSNF drip tests is unknown and due to the large surface area introduced by the alteration products is probably very small compared with any colloids that would form. The even distribution of alteration products over the fuel surfaces in the ANL tests suggest that the groundwater dripped on fuel has contacted all the surfaces; there is no evidence of channeling on the fuel fragments.

Uncertainties caused by reconfiguration (e.g., changing sample retainers) and experimental problems (evaporation of leachate, spent fuel particles falling into leachate) have been clearly identified and discussed throughout the report and are clearly marked on data plots and data tables. For example, the data plots in Figures 2, 6, and 10 identify when the new gold mesh sample retainer was put in, when vessels went dry and when fuel fragments fell into the leachate. The amount of evaporation of leachate from the tests is reported in [Finch et al. 2002, Tables 8 to 18]. These tables show leachate volumes recovered during each sampling interval (Interval End Vol.), pH measured in the leachate and the total volume of leachate that would have been recovered ("expected") if all water injected during each test interval had been (based

on the nominal injection volume of 1.5 mL per week). The difference between volumes of leachate recovered and the expected volumes provide an indication of injection efficiency and vessel leakage during each test interval. The uncertainties from experimental reconfiguration and experimental problems should be treated on a sample by sample basis when using the data.

Another source of uncertainty related to the test configurations is caused by the fact that the tests are cooled from the 90°C test temperature to ambient laboratory temperature (around 25°C) for sampling. This procedure does not affect the total nuclide release or fractional release data, because any sorption or plating out of nuclides onto the steel vessel walls is captured in the acid strip procedure. However, this cooling may influence the leachate chemistry and the stability of colloids in solution. Thus, the measured nuclide concentrations may not accurately represent what the concentrations were at 90°C, as colloids may precipitate and aggregate upon cooling or the sorption to behavior on the stainless steel vessel may be enhanced. Thus, the data reported in Appendix 2 are free of assumptions about what the concentrations of any radionuclide might have been at any temperature besides ambient. Concentrations reported here are simply concentrations of radionuclides in an aqueous solution that has been in contact with a stainless steel vessel that had been cooled from 90°C to ambient over a relatively brief period (typically less than 30 minutes).

Some uncertainty in the reported data is also introduced by the fact that we do not directly measure some key experimental factors during the tests. The most important of these factors include pH and dissolved oxygen, which have been shown by Shoesmith (2000) to play important roles in the dissolution behavior of UO_2 and perhaps UO_2 spent fuels. These factors are known at the beginning of each test interval but their precise values or activities are uncertain during testing at 90°C. Additional discussion of these factors is found in the unsaturated UO_2 testing data report (Finch et al. 2002).

F. Data Verification

Data spreadsheets were verified according to ANL QA procedure, YMP-AP-005, "Administrative Procedure for Performance of Data Verifications."

IV. DISCUSSION

The following section discusses results on colloids from (A) unsaturated corrosion tests of commercial spent nuclear fuel and (B) saturated tests of uranium mineral phases. Background on the experiments and analytical techniques employed were presented in previous sections of this report.

A. CSNF Colloids Generated in Unsaturated Tests

Few colloids have been detected in the test solutions from unsaturated corrosion tests of commercial spent nuclear fuel under likely water contact scenarios at Yucca Mountain. Both dynamic light scattering (DLS) and filtration techniques used to characterize the colloids generated from the spent fuel tests gave consistent results. The results obtained from DLS will be discussed first.

The DLS results shown in Figure 3 represent the amount of colloids in the leachate from the commercial spent fuel tests on-going at Argonne National Laboratory (represented in Figure 3 according to fuel type: ATM-103, ATM-106, and ATM-109). No distinction was made in Figure 3 between the various corrosion tests (high drip, low drip, or humid air); nor between the ATM-109 fuel types (A, B, or C). The DLS measurements were made on an aliquot taken at a sampling period (represented as the total test duration for the fuel corrosion). While no distinction except for fuel type was made in Figure 3, all the individual DLS test results are listed in Appendix 1.

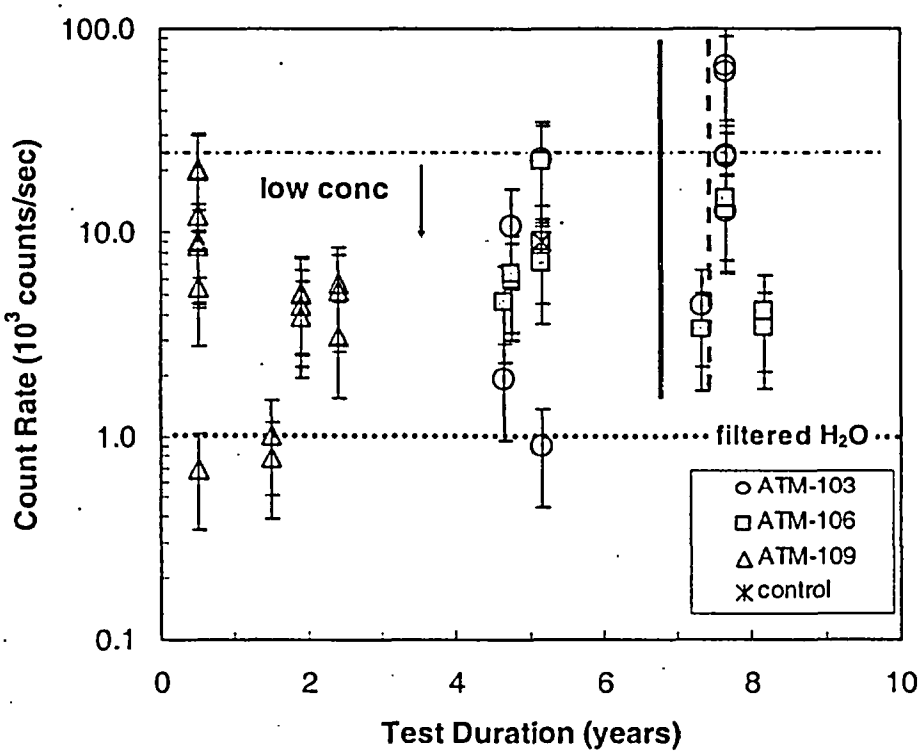

Figure 3. Relative amount of colloids present in leachates from commercial spent nuclear fuel tests sampled as a function of corrosion with EJ-13.
Note: The DLS results for the unsaturated drip tests are displayed for the ATM-103 (circle symbol), ATM-106 (square symbol), and ATM-109 (triangle symbols) fuels. The control tests for the ATM-103 and ATM-106 drip tests are displayed as the asterisk symbol. The solid (~6.8 yr) and dashed vertical lines (~7.3 yr) correspond to installation of a new zircaloy-4 retainer with 10 micron holes and a new gold screen with 200 micrometer holes, respectively.

As shown in Figure 3, the count rate is low (<30 kc/s) for the all of the unsaturated corrosion test leachates, except for one leachate at 7.7 years (ATM-103 HDR test). A low count rate indicates that particulates and/ or colloids are present in the leachate above the background of filtered water (< 1 kc/s). The count rate for the leachates from the 5.2 year ATM-103 high drip rate test and some of the ATM-109 tests were below the background for filtered water and thus colloids are not detected. Even the control test (test run with EJ-13 groundwater and no fuel) for the spent fuel unsaturated tests indicate a low count rate and the presence of particulate above the

background for filtered water. For the majority of the leachates analyzed for colloids using DLS, the size distribution was not resolved. Thus, even though a count rate above the background of filtered water indicates particulates are in the solution, the size distribution was not resolved with DLS due to the high polydispersity of the system and/or an unstable particulate suspension. While it is desirable to report a particle concentration for the spent fuel colloids, the conversion to a particle concentration from the DLS count rate is based upon the particle size and this was not possible for the majority of the leachates where the particle size was not resolved using DLS. Thus, the count rate for the CSNF leachates showed that only a small amount of particulate is present in the solutions above the background of filtered water.

The test configuration changes that occurred at 6.8 and 7.3 years (refer to Experimental Section for details) for the high drip rate ATM-103 and ATM-106 fuel tests were quite disruptive (fuel fragments and alteration products were transferred to new holder) and should have allowed a significant amount of colloidal material to be transported to the leachate. While the change to a new retainer with 10 micrometer holes and then later to a mesh with larger holes (200 micrometer holes) seemed to affect the amount of colloids and/ or particulate suspended in the leachate, the concentration remained low. The count rate for the samplings periods after the test configuration change was low and was similar to other sampling periods where the test configuration did not change. However, in one case, the count rate for the ATM-103 fuel high drip rate leachate at 7.7 years (after the 200 micron mesh test configuration change) indicated that some colloids were present and the size distribution was resolved (~150 nm) (See data in Appendix 1, Table A1-1). Since DLS is used to determine the size distribution of colloids and can not determine the composition of the colloids, ICP-MS and TEM are employed to get additional information about the colloids. Filtration results (from ICP-MS analyses) indicate that the uranium was associated with the particulate fraction (refer to the following section on ATM-103 colloids). As a low population of colloids was present, the composition of these colloids was not identified using TEM. These colloids appeared to be unstable and subsequently dropped to the very low concentration range when analyzed by DLS three months later.

Similar to the DLS results, very low concentrations of colloids were indicated from filtration results of plutonium and uranium concentrations in the leachates from the fuels tested under unsaturated conditions. The filtration results presented in this report focus on the U and Pu data since U is the primary constituent of the fuel and Pu is important for assessing the long-term performance of the fuel. The U and Pu concentrations associated with the colloidal fraction were bounded by the concentration in the unfiltered aliquot (supporting data is provided in the following section's discussion for the respective fuels).

Figure 4 shows the concentration of plutonium in the unfiltered leachate as a function of pH from all the fuels tested. No distinction was made in Figure 4 between the various corrosion tests (high drip, low drip, or humid air); nor between the ATM-109 fuel types (A, B, or C). The CSNF tests were run at 90°C and cooled to ambient laboratory temperature for sampling, thus literature data for Pu solubility in J-13 groundwater at 25 and 90°C is provided [Efurd]. For the majority of the CSNF fuel leachates, the plutonium concentration in the filtrates was bounded (set as an upper limit) by the Pu solubility limit in J-13 at 25° or 90°C or the concentration was below the detection limit for the alpha spectrometry or ICP-MS techniques. However, some Pu leachate concentrations were approximately an order of magnitude higher than the concentrations found in the majority of the tests and are at the solubility limit or supersaturated

for Pu in J-13. In these cases, the high Pu concentrations are explained by fragments of fuel that had been found in the leachate (fallen from the fuel retainer to the test solution at the base of the vessel). The filtration results from the high drip rate tests with the ATM-103 and ATM-106 fuels will be discussed in the following text. Only sporadic filtration data is available from the low drip rate and humid air CSNF tests; these will not be discussed here.

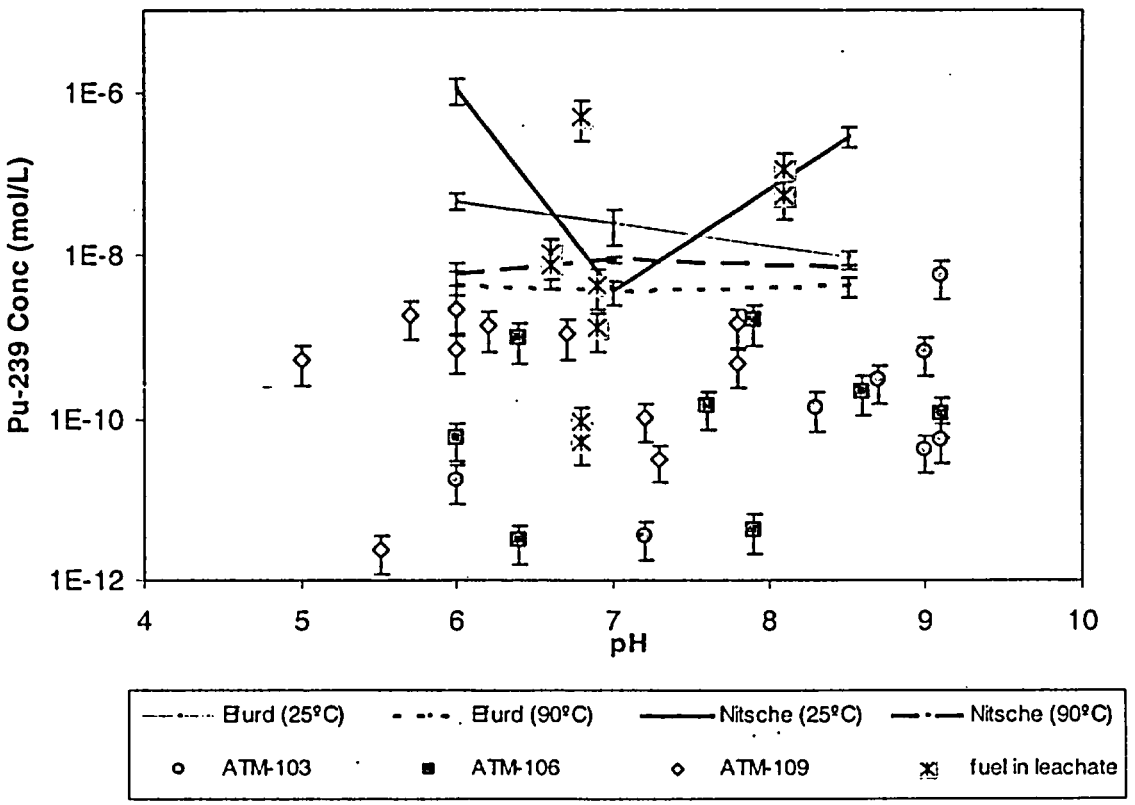

Figure 4. Plutonium concentration as a function of pH in unfiltered leachates from corrosion tests with CSNF.
Note: fuel in leachate = fuel fragments found in test solution.
Literature data for Pu in J-13 at 25 and 90°C [Efurd] is represented by the lines.

ATM-103 Fuel Colloids

The following section discusses results from high drip rate corrosion tests on the ATM-103 fuel. The high drip rate tests consistently had sufficient leachate available for colloidal analyses. The concentrations of U-238 and Pu-239 in the unfiltered leachates and filtrates from ATM-103 high drip rate corrosion tests are shown in Figure 5. (Data tables are given in Appendix 2.) The concentrations in the unfiltered leachates are an upper bound for the concentrations in the filtrates; the unfiltered leachates will be discussed first. The uranium concentration of the unfiltered leachate is on the order of 10^{-9} M at the 5.2 and 6.3 year samplings of the CSNF unsaturated tests (Figure 5a), while the samplings of the tests at 5.7, 7.3, 7.7, 8.2, and 8.7 are two to three orders of magnitude higher (uranium concentrations in the unfiltered leachate of 10^{-7} to 10^{-6} M; Figure 5a). It is important to note that test configuration changes to the spent fuel holder occurred at 6.8 and 7.3 years. Thus, the samplings at 7.3 and 7.7

years correspond to the leachates directly following the change to a new Zircaloy-4 retainer with 10 micrometer holes and then later to a gold-mesh with larger holes (200 micrometer holes), respectively. The highest concentration of U-238 corresponds to the holder change with the large diameter holes (new gold mesh retainer). While the test configuration changes can be used to explain the large releases, the relatively high concentration observed at 5.7 years (prior to the test holder change) is unexplained. The trends discussed above for U-238 were also observed for Pu-239 in the unfiltered leachates (Figure 5b). Next, the filtration data for uranium and plutonium will be discussed.

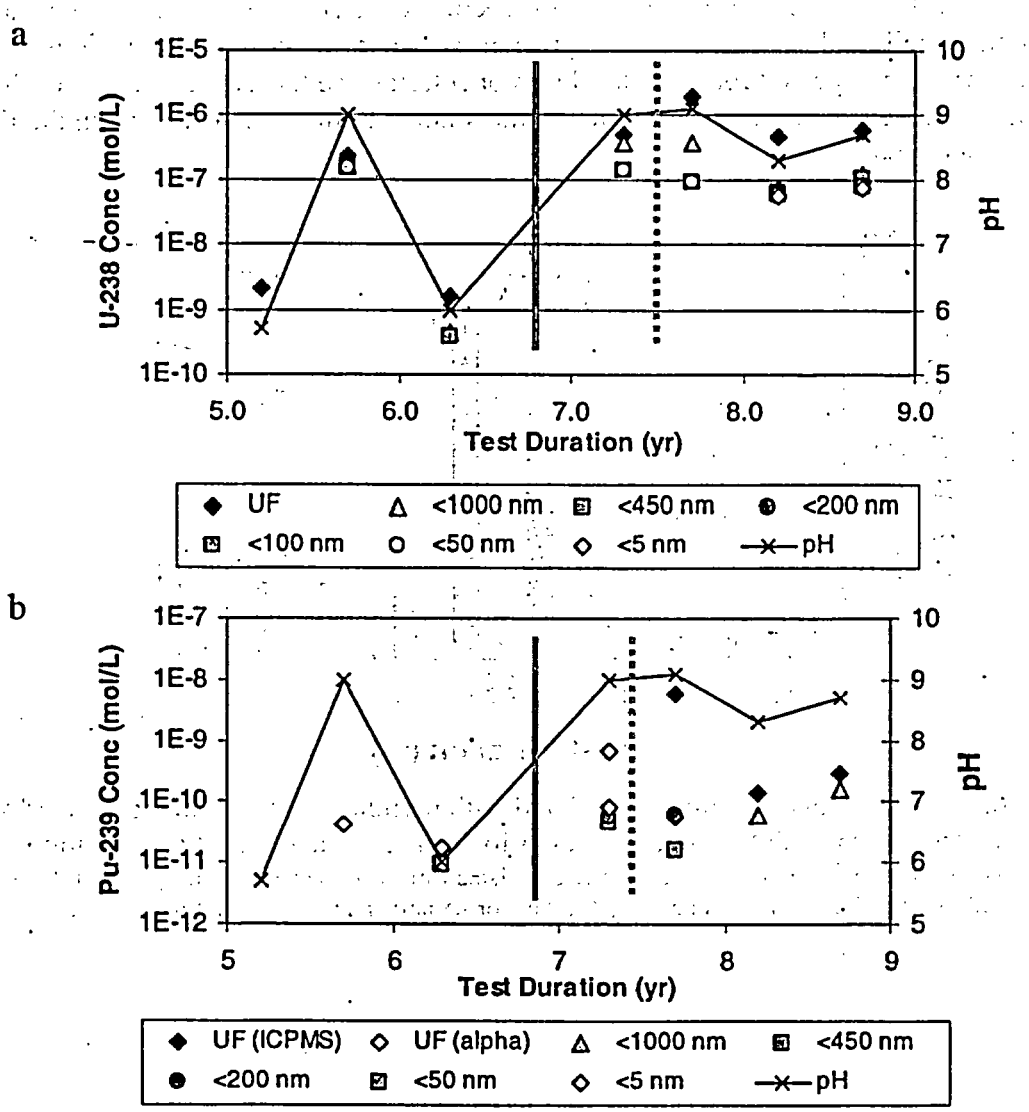

Figure 5. Concentration of (a) U-238 and (b) Pu-239, and pH of the test leachates as a function of test duration for the ATM-103 HDR test for sampling periods between 5.2 to 8.7 years. Note: Solid and open symbols are the unfiltered (UF) leachate and filtrate concentrations (see legend). The pH is represented by the x symbols and the line. The solid (~6.8 yr) and dashed vertical lines (~7.3 yr) correspond to installation of a new zircaloy-4 retainer with 10 micron holes and a new gold screen with 200 micrometer holes, respectively.

The concentration of U-238 and Pu-239 associated with various size fractions for the ATM-103 high drip rate corrosion test (HDR) sampled from 5.7 to 8.7 years is shown in Figure 6 and Table 6. The concentrations plotted in Figure 6 and the values in Table 6 were calculated from unfiltered leachates (UFL) and filtrate concentrations given in Finch 2002 (Appendix 2). As limited filtration data is available for Pu-239 (refer to Table 6), the U-238 data will be used predominantly to discuss the colloid releases. Filtration was not performed on the leachate from the 5.2 year sampling (one-third of the expected volume was recovered) and the vessel was dry at 6.8 years; thus no data is available for these sampling periods. While data for other uranium isotopes (U-234, U-235, and U-236) is available (Finch 2002), it is not presented here. The data presented for the U-238 size fractions in this section were consistent with the speciation (particulate, colloidal, and dissolved species) of the other uranium isotopes. No isotopic differences were expected for these leachates or filtrates and the concentrations of the uranium isotopes in the leachates are proportional to the amount in the fuel. The data on the filtrates will be discussed next.

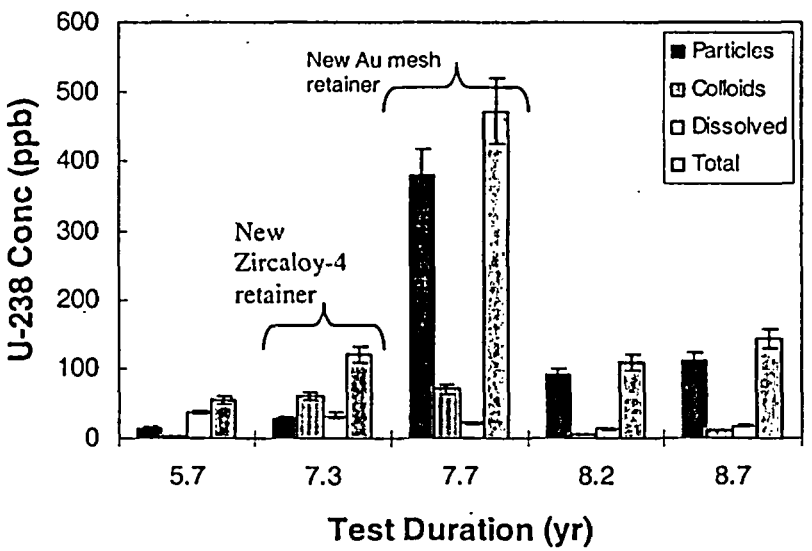

Figure 6. Uranium concentrations associated with particles, colloids, and dissolved species in leachates from ATM-103 HDR corrosion tests as a function of test duration.
Note: Concentration of the species were calculated from size fractions: $Conc_{particles}$ (>1000 nm), $Conc_{colloids}$ (50-1000 or 5-1000 nm), $Conc_{dissolved}$ (<50 nm or <5 nm) and $Conc_{Total}$ (unfiltered aliquot).

Table 6. Uranium and plutonium concentrations associated with various size fractions (particles, colloids, and dissolved) in leachates from ATM-103 HDR corrosion tests as a function of test duration.

Test Duration (yr)	$Conc_{particles}$ (ppb)	$Conc_{colloids}$ (ppb)	$Conc_{dissolved}$ (ppb)	$Conc_{particles}$ (ppb)	$Conc_{colloids}$ (ppb)	$Conc_{dissolved}$ (ppb)
Isotope	U-238	U-238	U-238	Pu-239	Pu-239	Pu-239
5.7	14	2.8	37	--	--	--
6.3	--	--	--	0.0019*	--	0.0023
7.3	28	60	33	0.15	0	0.019
7.7	380	71	22	--	--	--
8.2	91	4.9	13	--	--	--
8.7	110	12	18	--	--	--

Note: Concentration of the species were calculated from size fractions: $Conc_{particles}$ (>1000 or 450 nm), $Conc_{colloids}$ (50-1000 or 5-1000 nm), $Conc_{dissolved}$ (<50 nm or <5 nm). See Table 7 for filters sizes employed for filtration.

* This value is the concentration associated with particles + colloids, as UFL was used to calculate the concentration.

The uranium concentrations in filtrates from the 5.7 year sampling indicated that the main fraction was dissolved (70%) and a minor fraction was colloidal (~5%). At the 7.3 year sampling (first sampling subsequent to the placement of the new zircaloy-4 holder), approximately 50% of the uranium was in the colloidal fraction. The uranium concentration in the leachates after the test configuration change to the gold mesh retainer was dominated by the particulate fraction (represented by the difference between the concentration for the UFL and 1000 nm filter), where for these test sampling periods approximately 80% of the filtered uranium was the particulate fraction. The remaining 20% of the uranium was distributed almost evenly between the dissolved (represented by the concentration from the smallest filter) and colloidal fractions (represented by difference between the concentration for the largest and the smallest filters; refer to Table 6).

The importance of the colloids in the leachate was indicated by the ratio of the uranium concentration in solution after filtration through the largest filter ($Conc_{Coll+Diss}$) and the concentration from filtration through the smallest filter ($Conc_{Diss}$). Table 7 summarizes the colloid fraction for U-238 and Pu-239 being retained by the smallest filter. If no colloids are detected, this ratio is one. The filter sizes for the colloid and dissolved species varied for the test samplings. Filter sizes employed for the samplings are listed in Table 7. The dissolved fraction was <50 nm or <5 nm and the colloid fraction was one of the following ranges: 5-1000, 5-450, 50-1000, or 50-UFL. These definitions were based upon experimental constraints of available filters. Values for $Conc_{Coll+Diss} / Conc_{Diss}$ were approximately one for most of the ATM-103 HDR corrosion tests. In the one case (at 7.3 years) where the U-238 and Pu-239 ratios can be compared, the ratio for the colloid fraction for U-238 and Pu-239 differ by a factor of three, indicating that sorption or self-coagulation of Pu-239 with particles >450 nm on the 450 nm filter membrane may have occurred. The 7.7 year sampling period had a factor of four increase in the uranium concentration associated with colloids and the increase corresponded to the test configuration change (placement of the new gold mesh retainer).

Table 7. Colloid fraction determined from ratio of nuclide concentration in ATM-103 HDR leachates after filtration through large and small filters as a function of test duration.

Test Duration (yr)	$Conc_{Coll+Diss}$ / $Conc_{Diss}$	Large/Small Filter Sizes (nm)	$Conc_{Coll+Diss}$ / $Conc_{Diss}$	Large/Small Filter Sizes (nm)
Isotope	U-238	U-238	Pu-239	Pu-239
5.7	1.1	1000/50	--	--
6.3	--	--	<1*	UFL/50
7.3	2.8	1000/50	<1	450/5
7.7	4.3	1000/50	--	--
8.2	1.4	1000/5	--	--
8.7	1.6	1000/5	--	--

Note: Concentration of the species were calculated from size fractions in Table 6.
$Conc_{Coll+diss}$ = concentration in filtrate from largest filter used.
$Conc_{Diss}$ = concentration in filtrate from smallest filter used.
* This ratio includes a contribution from particulate as the UFL was used to calculate the ratio.

ATM-106 Fuel Colloids

The following section discusses results from high drip rate corrosion tests on the ATM-106 fuel, as the high drip rate tests consistently had sufficient leachate available for colloidal analyses. The concentrations of U-238 and Pu-239 in the unfiltered leachates and filtrates from ATM-106 high drip rate corrosion tests are shown in Figure 7. (Data tables are given in Appendix 2.) The concentrations in the unfiltered leachates are an upper bound for the concentrations in the filtrates; the unfiltered leachates will be discussed first. The uranium concentration of the unfiltered leachate is on the order of 10^{-8} M at the 6.3 and 6.8 year samplings of the CSNF unsaturated tests (Figure 7a), while the samplings of the tests at 5.7, 7.3, 8.2, and 8.7 are an order of magnitude higher (uranium concentrations in the unfiltered leachate of 10^{-7}; Figure 7a). It is important to note that test configuration changes to the spent fuel holder occurred at 6.8 and 7.3 years. Thus, the samplings at 7.3 and 7.7 years correspond to the leachates directly following the change to a new Zircaloy-4 retainer with 10 micrometer holes and then later to a gold-mesh with larger holes (200 micrometer holes), respectively. The highest concentration of U-238 (1×10^{-6} M, Figure 7a) corresponds to the sampling at 5.2 years (prior to the test configuration changes) and the high uranium concentration is unexplained at this time. The next highest concentration of U-238 in the unfiltered leachate (7×10^{-7} M, Figure 7a) corresponds to the placement of the new gold-mesh retainer with the large diameter holes. The trends discussed above for U-238 were also observed for Pu-239 in the unfiltered leachates (Figure 7b). Next, the data for uranium and plutonium concentrations in filtrates will be discussed.

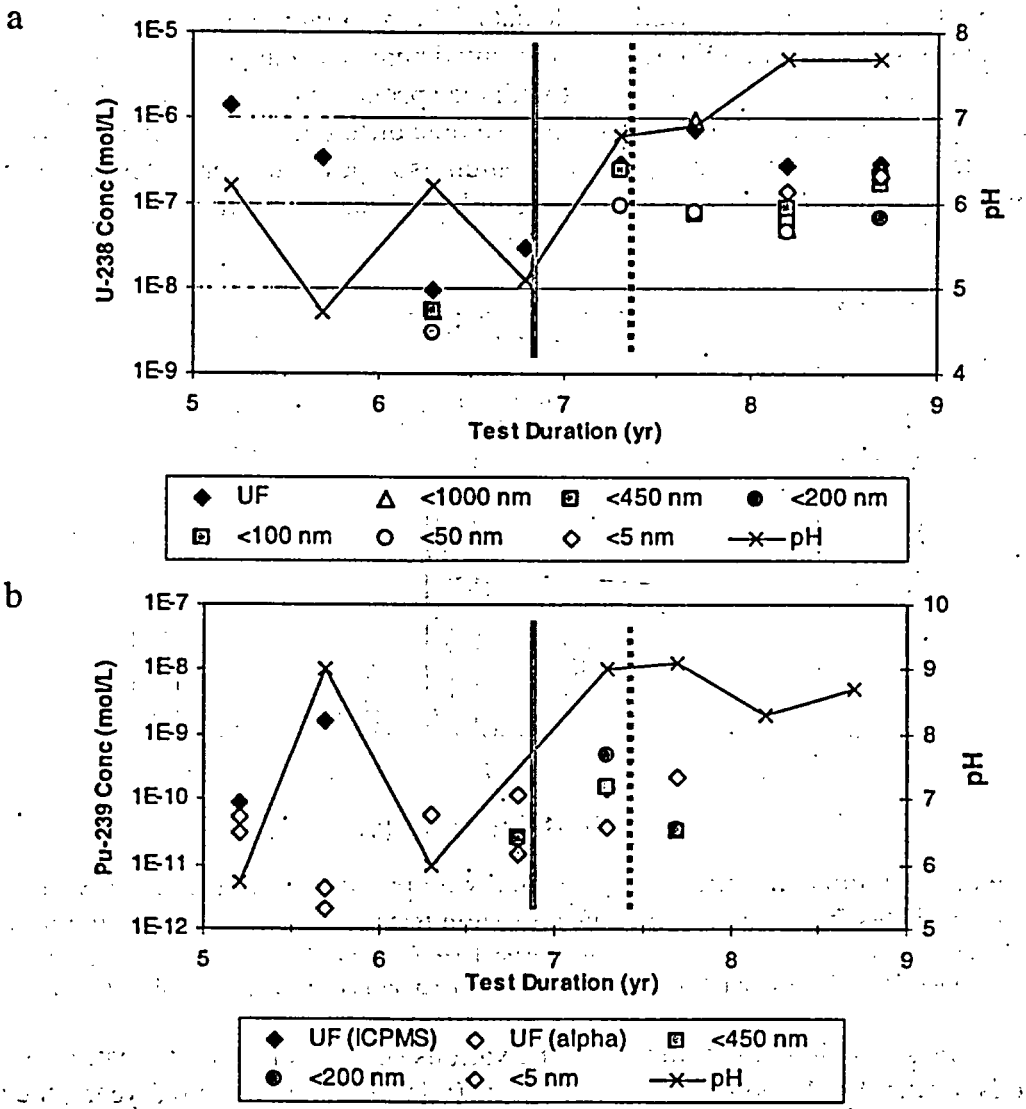

Figure 7. Concentration of (a) U-238 and (b) Pu-239, and pH of the test leachates as a function of test duration for the ATM-106 HDR test for sampling periods between 5.2 to 8.7 years. Note: Solid and open symbols are the unfiltered (UF) leachate and filtrate concentrations. The pH is represented by the x symbols and the line. The solid (~6.8 yr) and dashed vertical lines (~7.3 yr) correspond to installation of a new zircaloy-4 retainer with 10 micron holes and a new gold screen with 200 micrometer holes, respectively.

The concentration of U-238 and Pu-239 associated with various size fractions for the ATM-106 high drip rate corrosion test (HDR) sampled from 6.3 to 8.7 years is shown in Figure 8 and Table 8. The concentrations plotted in Figure 8 and the values in Table 8 were calculated from unfiltered leachate (UFL) and filtrate concentrations given in elsewhere (Appendix 2 in Finch 2002). As limited filtration data is available for Pu-239 (refer to Table 8), the U-238 data will be used predominantly to discuss the colloid releases. Filtrates were not submitted for ICP-MS analyses for the 5.2 and 6.8 year samplings where significant volumes losses occurred in the tests (only one-third and one-tenth of the expected volumes were recovered at 5.2 and 6.8 year samplings, respectively); thus no U-238 data is available for these sampling periods. In addition, filtrates were not submitted for ICP-MS analyses for the 5.7 year sampling, and no U-238 data is

available for this sampling period. While data for other uranium isotopes (U-234, U-235, and U-236) is available (Finch 2002), it is not presented here. The data presented for the U-238 size fractions in this section were consistent with the speciation (particulate, colloidal, and dissolved species) of the other uranium isotopes. No isotopic differences were expected for these leachates or filtrates and the concentrations of the uranium isotopes in the leachates are proportional to the amount in the fuel. The data on the filtrates will be discussed next.

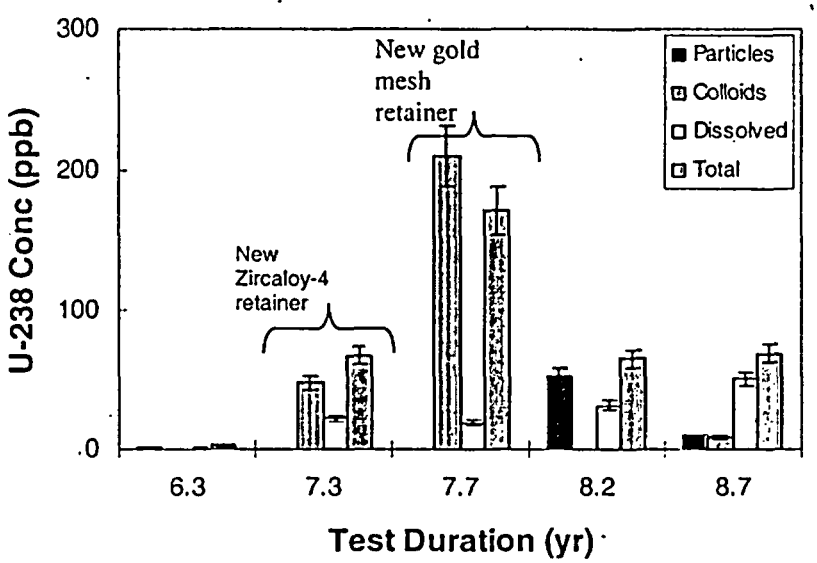

Figure 8. Uranium concentrations associated with particles, colloids, and dissolved species in leachates from ATM-106 HDR corrosion tests as a function of test duration.
Note: Concentration of the species were calculated from size fractions: $Conc_{particles}$ (>1000 nm), $Conc_{colloids}$ (50-1000 or 5-1000 nm), $Conc_{dissolved}$ (<50 nm or <5 nm) and $Conc_{Total}$ (unfiltered aliquot).

The speciation of uranium from the various sized filters varied greatly between sampling periods for the ATM-106 HDR corrosion tests (refer to Table 8). At 6.3 years, the uranium concentration was low and was almost evenly distributed between the particulate, colloidal and dissolved fractions (25-45%). The samplings at 7.3 and 7.7 years correspond to the leachates directly following the change to a new retainer with 10 micrometer holes and then later to a mesh with larger holes (200 micrometer holes) (refer to Section II.A.1 for details). At the 7.3 year sampling (first sampling subsequent to the placement of the new zircaloy-4 holder), approximately 70% of the uranium was in the colloidal fraction and 30% was in the dissolved fraction. The uranium concentration in the leachates after the test configuration change to the gold mesh retainer (7.7 year sampling) was also dominated by the colloidal fraction (~90%) with the remaining 10% of the uranium present as dissolved species less than 50 nm (refer to Figure 8 and Table 8. While the concentration of uranium in the unfiltered leachate increased subsequent to the test configuration changes (refer to Figure 7a at 7.3 and 7.7 year samplings), the concentration of uranium is less than or equal to the uranium concentration at samplings prior to the test configuration changes(5.2 and 5.7 year samplings). No speciation data was available for U-238 for the 5.2 and 5.7 year samplings, but Pu-239 data is available from alpha spectrometry analyses. Based upon the Pu-239 associated with various species (particulate, colloidal, and dissolved), the Pu-239 is evenly distributed between the particulate and/ or colloids (>5 nm

fraction) and dissolved species for the 5.2 and 5.7 year samplings. While the test configuration change appears to have caused the increase in the release of colloids, the other samplings periods (refer to 5.2 and 5.7 year samplings in Figure 7a) with similar or higher uranium concentrations in the unfiltered leachate are not be explained at this time. Sampling periods following the test configuration changes resulted in significantly less colloidal material being released. At 8.2 years, approximately 60% of the uranium in solution was found as particulate (>1000 nm), none in the colloidal fraction, and 40% as the dissolved fraction. At 8.7 years, ~70% of the uranium in the leachate was in the dissolved fraction.

Table 8. Uranium and plutonium concentrations associated with various size fractions (particles, colloids, and dissolved) in leachates from ATM-106 HDR corrosion tests as a function of test duration.

Test Duration (yr)	$Conc_{particles}$ (ppb)	$Conc_{colloids}$ (ppb)	$Conc_{dissolved}$ (ppb)	$Conc_{particles}$ (ppb)	$Conc_{colloids}$ (ppb)	$Conc_{dissolved}$ (ppb)
Isotope	U-238	U-238	U-238	Pu-239	Pu-239	Pu-239
5.2	--	--	--	0.0052 (a)*; 0.014 (i)*	--	0.0073
5.7	--	--	--	0.00054 (a)*; 0.38 (i)*	--	0.00047
6.3	0.95	0.56	0.70	--	--	--
6.8	--	--	--	0.022	0.0026	0.0035
7.3	0	48	22	--	--	--
7.3	--	--	--	0	0.029	0.0088
7.7	0	210	19	--	--	--
8.2	53	0	32	--	--	--
8.7	9.6	8.6	51	--	--	--

Note: Concentration of the species were calculated from size fractions: $Conc_{particles}$ (>1000 or 450 nm), $Conc_{colloids}$ (50-1000 or 5-1000 nm), $Conc_{dissolved}$ (<50 nm or <5 nm). See Table 7 for filters sizes employed in filtration. Shaded cells indicate that fuel was found in leachate at test sampling.

*This value is the concentration associated with particles + colloids

(a) alpha spectrometry data

(i) ICP-MS data

As previously discussed for the ATM-103 HDR tests, the importance of the colloids in the leachate was indicated by the ratio of the uranium concentration in solution after filtration through the largest filter ($Conc_{Coll+Diss}$) and the smallest filter ($Conc_{Diss}$). Table 9 summarizes the colloid fraction from ATM-106 HDR tests for U-238 and Pu-239 being retained by the smallest filter. If no colloids are detected, this ratio is one. The filter sizes for the colloid and dissolved species varied for the test samplings. Filter sizes employed for the samplings are listed in Table 9. The dissolved fraction was <50 nm or <5 nm, and the colloid fraction was one of the following ranges: 5-1000, 5-450, 50-1000, or 50-UFL. These definitions were based upon experimental constraints of available filters. Values for $Conc_{Coll+Diss}$ / $Conc_{Diss}$ were approximately 1-3 for most of the ATM-103 HDR corrosion tests. In the one case (at 7.3 years) where the U-238 and Pu-239 ratios can be compared, the ratio for the colloid fraction for U-238 and Pu-239 are in good agreement (3.2 versus 2.1, respectively), indicating that the U and Pu are associated with the same species in the leachate. The 7.7 year sampling period had a factor of 12

increase in the uranium concentration associated with colloids and the increase corresponded to the test configuration change (placement of the new gold mesh retainer). These colloids were low in concentration based upon DLS results (count rate of 13-15 kc/s from Appendix 1, Table A1-3). At the 5.2 year sampling, the ratios for Pu-239 from two different analysis techniques (alpha spectrometry and ICP-MS) are in good agreement. However, the ratio for the colloid fraction at the 5.7 year sampling determined from ICP-MS analysis is higher than the ratio from alpha spectrometry by 400 times. The value from the ICP-MS analysis appears to be highly questionable, since the ratio for the colloid fraction determined from alpha spectrometry analyses is consistent with ratios from other sampling periods.

Table 9. Colloid fraction determined from ratio of nuclide concentration in ATM-106 HDR leachates after filtration through large and small filters as a function of test duration.

Test Duration (yr)	$Conc_{Coll+Diss}$ / $Conc_{Diss}$	Large/Small Filter Sizes (nm)	$Conc_{Coll+Diss}$ / $Conc_{Diss}$	Large/Small Filter Sizes (nm)
Isotope	U-238	U-238	Pu-239	Pu-239
5.2	--	--	1.7 (a)*; 2.9 (i)*	UFL/5
5.7	--	--	2.1 (a)*; 810 (i)*	UFL/5
6.3	1.8	1000/50	--	--
6.8	--	--	1.7	450/5
7.3	3.2	1000/50	--	--
7.3	--	--	2.1	450/5
7.7	12	1000/50	--	--
8.2	<1	1000/5	--	--
8.7	1.2	1000/5	--	--

Note: Concentrations of the species were calculated from size fractions in Table 8.
$Conc_{Coll+diss}$ = concentration in filtrate from largest filter used.
$Conc_{Diss}$ = concentration in filtrate from smallest filter used.
(a) alpha spectrometry data
(i) ICP-MS data
* This ratio includes a contribution from particulate as the UFL was used to calculate the ratio.

In summary, the release of particulate or colloids from the ATM-103 and ATM-106 HDR tests seems to correlate well with a disruptive event such as the test configuration change (placement of fuel in holders with new retainers of larger pore sizes). However, those colloids or particulate in the leachates subsequent to the test configuration changes are low in concentration. The stability of these phases is unknown at this time.

B. Uranium Mineral Phase Colloids under Saturated Conditions

As uranium-based spent nuclear fuels will be prevalent at the high-level waste repository at Yucca Mountain (oxidizing conditions), we have examined the colloidal properties of a mixture of two uranium minerals under saturated conditions that promote stable colloids. This section presents results of analyses on colloidal suspensions of meta-schoepite, $((UO_2)_4)(OH)_6 \cdot 5H_2O$, and UO_{2+x}, in 10 mM uranyl nitrate or J-13 groundwater (a 1 mg/mL suspension of the uranium minerals in 10 mM uranyl nitrate (pH 5.1) or a 0.2 mg/mL suspension in J-13 groundwater (pH 7.7). The uranyl nitrate solution (10 mM and pH 4.8) was chosen since it is within a stable region for the meta-schoepite mineral. A suite of techniques was used to

characterize the colloids including dynamic light scattering, transmission electron microscopy, and zeta potential measurements (additional details can be found in Mertz et al., 2002).

TEM micrographs of typical uranium-based colloids (either meta-schoepite or uranium dioxide) observed in solution from tests with the 10 mM uranyl nitrate and J-13 groundwater solutions appear in Figure 9. The crystalline phase of the colloids was identified using electron diffraction. These colloid phases were found to span a large range of sizes from nanometers to particles exceeding several micrometers in at least one dimension. Large 200 nm colloids of meta-schoepite and UO_{2+x} were dominant in the 10 mM uranyl nitrate suspension (Figure 9 a and b). The colloids detected in the tests with J-13 groundwater (Figure 9 c and d) exhibited two colloid types: large 100- to 200-nm UO_{2+x} colloids and needle-like colloids of meta-schoepite (with extremely fine microstructure exhibited for the meta-schoepite colloids). Some evidence of uranyl silicates was noted, although these phases were rare.

The meta-schoepite and uranium dioxide colloids in 10 mM uranyl nitrate were monitored in situ using DLS from the initial solution preparation until 100 days later for changes in the size and concentration of the colloids. Replicate measurements for the sizing and concentration measurements are shown in Figure 10. The size of the colloids remains constant over the time period (average size of 216 ± 23 nm and 206 ± 7 nm, at 1 and 101 days after sampling, respectively). In addition, the size distribution remained the same (polydispersity of 0.20 ± 0.04 and 0.20 ± 0.05, at 1 and 101 days, respectively). The concentration of uranium substrate colloids was estimated using the 100 nm PS NIST standard curve fit equation (based upon the curve in Figure 1) which will overestimate the concentration for the 200 nm uranium substrate colloids. However, the concentration of the colloids decreased steadily over the hundred days implying sedimentation or sorption of the colloids occurred, since the size distribution remained constant.

Zeta potential measurements were performed on the meta-schoepite and uranium dioxide suspension (mixture) in 10 mM uranyl nitrate and on UO_{2+x} colloids in 1 mM $NaClO_4$ (Figure 11) to determine the zeta potential as a function of pH. The zeta potential curve for the meta-schoepite + UO_{2+x} colloidal suspension is unstable with respect to the zeta potential (<20 mV) at pH values ≤ 5. The UO_{2+x} colloids maintain a large negative zeta potential over the pH range of 2 to 11.5 (solid squares in Figure 11), indicating a stable colloidal suspension with zeta potentials > 20 mV. The point of zero charge (PZC) for UO_2 in the literature (3 and 4.5) [Parks] is in good agreement with the pzc of 2 determined for UO_{2+x} in 1 mM $NaClO_4$. Zeta potential measurements for the meta-schoepite and UO_{2+x} suspension in 10 mM uranyl nitrate indicated that the colloids are not stable at pH values less than or equal to five. In this pH region (≤ 5), the zeta potential of the colloids is zero or slightly negative suggesting selective coagulation for a mixed colloidal suspension [Pugh]. A positive zeta potential for the meta-schoepite colloids could explain this behavoir and can be confirmed by zeta potential measurements on a suspension of meta-schoepite colloids. At pH values of 5.5 and higher, the meta-schoepite and UO_{2+x} colloids are stable and have zeta potential values of –30 to –60 mV. As a check of the stability and reproducibility of the ELS measurements, the zeta potential measurements were repeated at pH values of 5.5 and 7. The zeta potentials were in excellent agreement with measurements made one or two days earlier, thus indicating that the zeta potentials were reproducible and that the sample appeared to be stable.

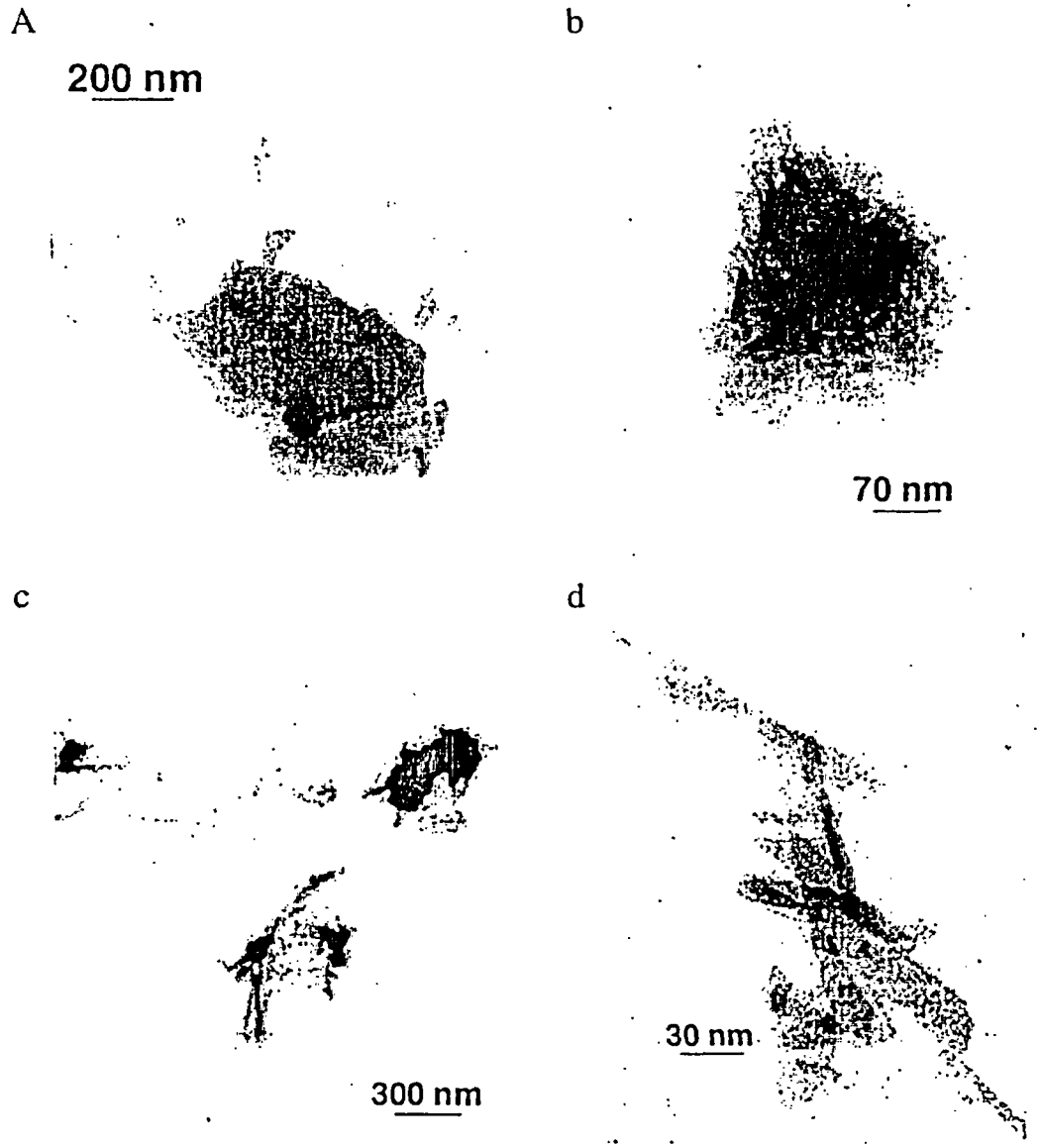

Figure 9. TEM micrographs of (a) metaschoepite and (b) uranium dioxide colloids from 10 mM uranyl nitrate, (c) metaschoepite (needle-like) and uranium dioxide (globular) colloids from J-13 groundwater, and (d) metaschoepite colloids from J-13 groundwater.

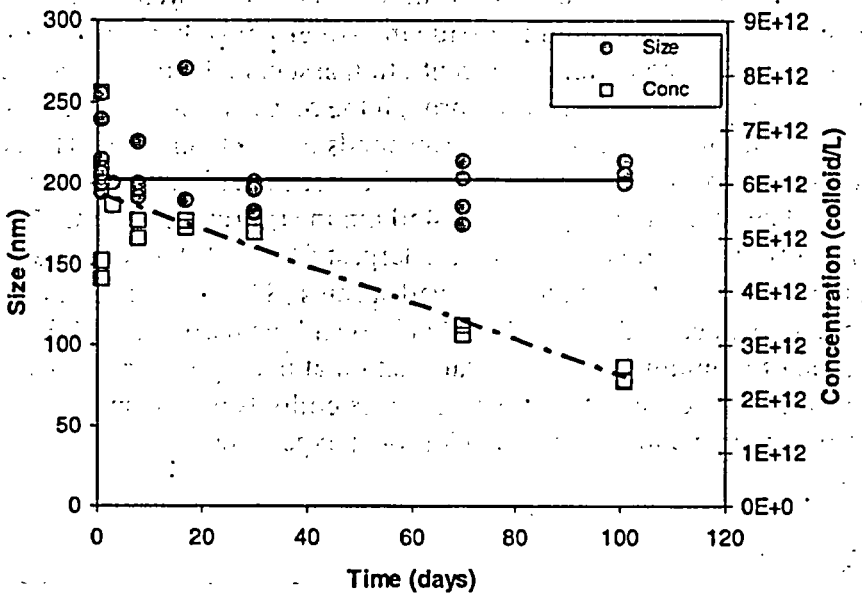

Figure 10. Colloid size (solid circles, solid line) and number concentration (open squares, dashed line) for meta-schoepite and UO_{2+x} suspension in 10 mM uranyl nitrate as a function of elapsed time from colloidal suspension preparation. Lines are drawn to show trends.

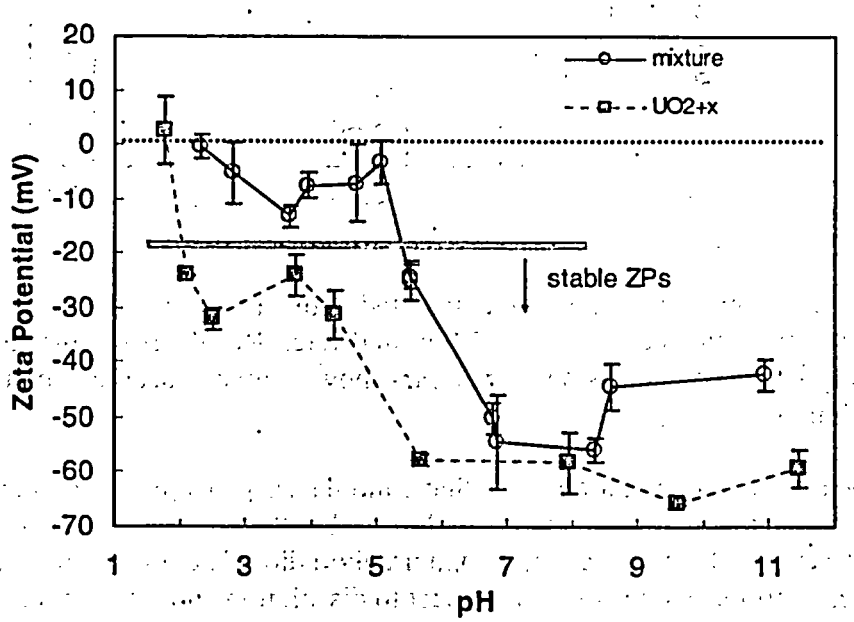

Figure 11. Zeta potential as a function of pH for a mixture of meta-schoepite and UO_{2+x} colloids in 10 mM uranyl nitrate (open circles, solid line) compared with UO_{2+x} colloids in 1 mM $NaClO_4$ (solid squares, dashed line). Error bars show standard deviation from multiple measurements.

As the colloids observed by TEM in this study were uranium substrate colloids, filtrates of the meta-schoepite and uranium dioxide in J-13 groundwater suspension were analyzed using ICP-MS to determine the uranium concentration associated with the various size fractions (Figure 12). The uranium that passed through the 5,000 nominal molecular weight filter is considered the dissolved fraction and corresponds to less than 2 nm. The colloidal fraction for these tests is defined as the uranium fraction between 2 and 450 nm. While uranium associated with a particulate fraction is greater than 450 nm in size (as with the CSNF tests, this is an operational definition and is limited by the largest filter). Of the total uranium present in solution, the largest fraction is the dissolved species (84%). Much smaller percentages of uranium are associated with the colloidal (12%) and the particulate (4%) fractions. The concentration of uranium in the colloidal fraction at 670 ppb appears to allow easy detection of colloids by TEM. The stability of these of these colloids with respect to dissolution or agglomeration can be confirmed with additional experiments.

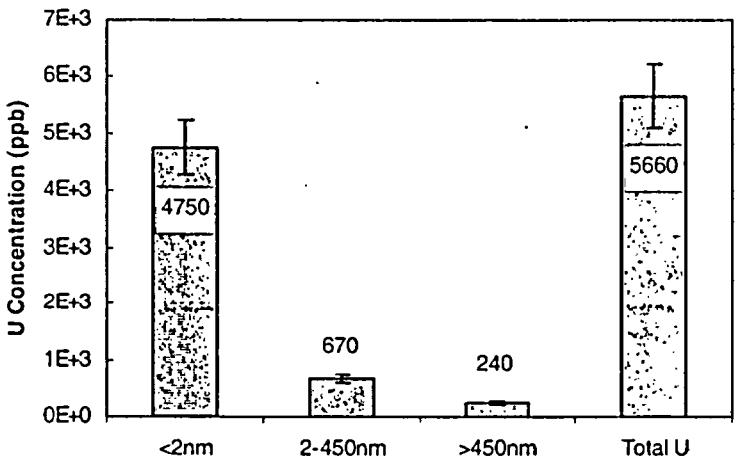

Figure 12. Concentration of uranium associated with various size fractions from a suspension of meta-schoepite and UO_{2+x} in J-13 groundwater. Results from filtration and ICPMS analyses of the suspension. Error bars show estimated accuracy of 10% for the ICPMS technique.

The results in this section show that colloidal suspensions of uranium substrate colloids are possible under repository relevant conditions, but the uranium speciation is dominated by the dissolved fraction. The meta-schoepite and uranium dioxide colloids presented in this paper are stable under short duration tests with respect to dissolution and interparticle interactions at near neutral and higher pH values. The size and concentration of the colloids can be used in transport models to suggest potential transport of these species in the subsurface. Additional characterization of these colloids and their long-term stability under various repository relevant scenarios are warranted.

REFERENCES

E.C. Buck and J.K. Bates (1999) "Microanalysis of Colloids and Suspended Particles from Nuclear Waste Glass Alteration," *Applied Geochemistry*, 14, 635-653.

J.C. Cunnane (2001) "YMP Guidelines Concerning Measurement Uncertainties." ANL QA # YMP-12-469.

CRWMS M&O (2000) Commercial Spent Nuclear Fuel Degradation in Unsaturated Drip Tests. Input Transmittal WP-WP-99432.T. Las Vegas, Nevada: CRWMS M&O ACC: MOL.20000107.0209.

W. L. Ebert and J. K. Bates (1993) "A Comparison of Glass Reaction at High and Low Glass Surface/Solution Volume," *Nuclear Technology*, 104, 372-384.

D.W. Efurd, W. Runde, J.C. Banar, D.R. Janecky, J.P. Kaszuba, P.D. Palmer, F.R. Roensch, and C.D. Tait (1998) *Environ. Sci. Technol.*, 32, 3893.

R.J. Finch, J.L. Jerden, Jr., C.J. Mertz, Y. Tsai, J.C. Cunnane, and P.A. Finn (2002) "Unsaturated Testing of Bare UO2 Fuel Fragments: Data Report," YMP Activity PAWC1M5.

P. A. Finn, E. C. Buck, M. Gong, J. C. Hoh, J. W. Emery, L. D. Hafenrichter, and J. K. Bates, (1994) "Colloidal Products and Actinide Species in Leachate from Spent Nuclear Fuel," *Radiochem, Acta*, 66/67, 189-195.

Geckeis, H., Grambow, B., Loida, A., Luckscheiter, B., Smailos, E., and Quinones, J. (1998) "Formation and Stability of Colloids under Simulated Near Field Conditions," *Radiochem. A*cta, 82, 123-128.

R. J. Guenther, D.E. Blahnik, T.K. Campbell, U.P. Jenquin, J.E. Mendel, L.E. Thomas, and C.K. Thornhill (1988a) "Characterization of Spent Fuel: Approved Testing Material – ATM-103," PNL-5109-103, April 1988, Richland, WA.

R. J. Guenther, D.E. Blahnik, T.K. Campbell, U.P. Jenquin, J.E. Mendel, and C.K. Thornhill (1988b) "Characterization of Spent Fuel: Approved Testing Material – ATM-106," PNL-5109-106; October 1988, Richland, WA.

C. H. Ho and N. H. Miller (1986) "Formation of Uranium Oxide Sols in Bicarbonate Solutions," *J. Colloid Interface Sci.*, 113, 232-240.

A.B. Kersting, D.W. Efurd, D.L. Finnegan, D.J. Rokop, D.K. Smith, and J.L. Thompson, (1999) "Migration of Plutonium in Ground Water at the Nevada Test Site," *Nature*, 397, 56-59.

J.J. Lenhart and J.E. Saiers (2002) "Transport of Silica Colloids through Unsaturated Porous Media: Experimental Results and Model Comparisons," *Environ. Sci. Technol.* 36, 769-777.

C.J. Mertz, J.A. Fortner, and Y. Tsai (2002) "Understanding the Behavior and Stability of Some Uranium Mineral Colloids," Mater. Res. Soc. Proc., Fall 2002, Boston, MA, Submitted for publication.

N. Miekeley, H. Coutinho de Jesus, C. L. Porto da Silveira, and C. Degueldre (1992) *J. Geochem. Explor.*, 45, 409.

G.A. Parks (1964) "The Isoelectric Points of Solid Oxides, Solid Hydroxides, and Aqueous Hydroxo Complex Systems," 177-198.

R.J. Pugh (1992) "Selective Coagulation of Colloidal Mineral Particles," Colloid Chemistry in Mineral Processing, Vol. 12, Eds. J.S. Laskowski and J. Ralston, New York, NY: Elsevier, 268-271.

M. K. Schultz, "Sample Preparation for Low-Level Alpha-Spectrometry- Air Filters, Water, and Soils," ORTEC Technical Specifications and Recommendations.

P. Schurtenberger and M.E. Newman (1993) "Characterization of Biological and Environmental Particles Using Static and Dynamic Light Scattering," Environmental Particles, Vol. 2, J. Buffle and H.P. vanLeeuwen, Eds., Lewis Pub., Boca Raton, FL 37-115.

S.A. Short, R.T. Lowson, and J. Ellis (1988) *Geochimica et Cosmochimica Acta*, **52**, 2555.

S. Veerapaneni, J. Wan, and T.K. Tokunaga (2000) "Motion of Particles in Film Flow," *Environ. Sci. Technol.* 34, 2465-2471.

J. Wan and T.K. Tokunaga (1997) "Film Straining of Colloids in Unsaturated Porous Media: Conceptual Model and Experimental Testing," *Environ. Sci. Technol.* 31, 2413-2420.

J. Wan and J.L. Wilson (1994) "Colloid Transport in unsaturated porous media," *Water Resources Res.* 30, 857-864.

S.F. Wolf, D.L. Bowers, and J.C. Cunnane (2000) "Analysis of Spent Nuclear Fuel Samples from Three Mile Island and Quad Cities Reactors: Final Report" Chemical Technology Division, Argonne National Laboratory. YMP Data Report, ANL QA # YMP/SF-3A-319.

Appendix 1

Table A1-1. Summary of DLS Analyses on Leachates from ATM-103 Spent Fuel Corrosion Tests

Waste Form	Test Duration (months)	Test Type	Test Duration (yr)	Sample ID	Summary of DLS Analyses: Size[a] (nm)	Count Rate[b] (kcts)	Conc[c] (particles/L)	Size Std Equation[d]	Data Reference: DLS Reference	SNL page	Comments
ATM-103	prior to 56	all	prior to 4.7	--	--	--	--	--	--	--	aliquots not available for DLS prior to 4.7 yr
ATM-103	56	low drip	4.7	S31J-56	NR	--	--	--	S31J56.dat	1381/90	
ATM-103	56	vapor	4.7	S3V - 56	NR	1.9	--	--	S3V56.dat	1381/83-85	
ATM-103	57	high drip	4.8	S32J - 57	NR	10.8	--	--	S32J57.dat	1381/89	
ATM-103	62	high drip	5.2	S32J - 62	NR	0.9	--	--	S32J62.dat	1381/172	
ATM-103	62	vapor	5.2	S3V - 62	NR	23.1	--	--	S3V62.dat	1381/172,173	
ATM-103	69	low drip	5.8	S31J - 69	--	--	--	--	--	--	
ATM-103	69	high drip	5.8	S32J -69	--	--	--	--	--	--	
ATM-103	75	high drip	6.3	S32J - 75	--	--	--	--	--	--	
ATM-103	88	high drip	7.3	S32J - 88	NR	4.399	--	--	Finn0600.sz2	1644/68	
ATM-103	92	high drip	7.7	S32J -92	NR	12.728	--	--	Finn1000.sz2	1644/115-116	monitored aliquot @ 8 days after sampling
ATM-103	92	high drip	7.7	S32J -92	161.4	61.3	2.452E+12	100 nm NIST	Finn1000.sz2	1644/115-116	monitored aliquot @ 8 days after sampling
ATM-103	92	high drip	7.7	S32J -92	150.0	66.3	2.652E+12	100 nm NIST	Finn1000.sz2	1644/115-116	monitored aliquot @ 8 days after sampling
ATM-103	92	high drip	7.7	S32J -92	--	23.6	9.44E+11	100 nm NIST	Finn1000.sz2	1644/115-116	monitored aliquot @ 9 days after sampling
ATM-103	92	high drip	7.7	S32J -92	139.5	--	--	--	Finn1000.sz2	1644/115-116	monitored aliquot @ 9 days after sampling
ATM-103	92	high drip	7.7	S32J -92	168.3	--	--	--	Finn1000.sz2	1644/115-116	monitored aliquot @ 9 days after sampling
ATM-103	92	high drip	7.7	S32J -92	--	23.8	9.52E+11	100 nm NIST	PF061401.sz2	1644/115-116	monitored aliquot @ 91 days after sampling
ATM-103	92	high drip	7.7	S32J -92	173.5	--	--	--	PF061401.sz2	1644/115-116	monitored aliquot @ 91 days after sampling
ATM-103	92	high drip	7.7	S32J -92	158.2	--	--	--	PF061401.sz2	1644/115-116	monitored aliquot @ 91 days after sampling
ATM-103	98	high drip	8.2	S32J -98	NR	4.23	--	--	PF041801.sz2	1644/164	
ATM-103	98	high drip	8.2	S32J -98	NR	3.884	--	--	PF041801.sz2	1644/164	

NR size distribution not resolvable using DLS

-- not available or not analyzed

a Average colloid size determined by DLS

b Count rate determined using laser power of 3 mW (514.5 nm argon ion laser)

c Concentration calculated from count rate (at 3 mW) using equation for PS size standard indicated in Size Std Equation column.

d Equation for size standard that is closest in size to the spent fuel colloids (thus only for colloid sizes resolved by DLS).

Appendix 1

Table A1-2. Summary of DLS Analyses on Leachates from Control Tests for ATM-103 and ATM-106

Waste Form	Test Duration (months)	Test Type	Test Duration (yr)	Sample ID	Summary of DLS Analyses: Size[a] (nm)	Count Rate[b] (kc/s)	Conc[c] (particles/L)	Size Std Equation[d]	Data Reference: DLS Reference	SN I page	Comments
control		all	prior to 4.7	–	–	–	–	–	–	–	aliquots not available for DLS prior to 4.7 yr
control	56	control	4.7	CC1J-56	NR	–	–	–	CC1J56.dat	1381/84-85	
control	62	control	5.2	CC1J-62	NR	9.0	–	–	CC1J62.dat	1381/172,173	
control	69	control	5.8	CC1J-69	–	–	–	–	–	–	

NR size distribution is not resolvable

– not available or not analyzed

a Average colloid size determined by DLS

b Count rate determined using laser power of 3 mW (514.5 nm argon ion laser)

c Concentration calculated from count rate (at 3 mW) using equation for PS size standard indicated in Size Std Equation column.

d Equation for size standard that is closest in size to the spent fuel colloids (thus only for colloid sizes resolved by DLS).

Appendix 1

Table A1-3. Summary of DLS Analyses on Leachates from ATM-106 Spent Fuel Corrosion Tests

Waste Form	Test Duration (months)	Test Type	Test Duration (yr)	Sample ID	Summary of DLS Analyses: Size[a] (nm)	Count Rate[b] (kc/s)	Conc[c] (particles/L)	Size Std Equation[d]	Data Reference: DLS Reference	SN I page	Comments
ATM-106		all	prior to 4.7	--	--	--	--	--	--		aliquots not available for DLS prior to 4.7 yr
ATM-106	56	vapor	4.7	S6V - 56	330	4.6	2.76E+09	300 nm NIST	S6V56.dat	1381/83-85, 133-134,187-188	
ATM-106	56	low drip	4.7	S61J-56	NR	--	--	--	S61J56.dat	1381/84-85	
ATM-106	57	high drip	4.8	S62J - 57	NR	5.9	--	--	S62J57.dat	1381/89-90	
ATM-106	57	high drip	4.8	S62J - 57	NR	6.4	--	--	S62J57.dat	1381/89-90	
ATM-106	62	high drip	5.2	S62J - 62	NR	22.5	--	--	S62J62.dat	1381/172	
ATM-106	62	vapor	5.2	S6V - 62	NR	7.2	--	--	S6V62.dat	1381/172,173	
ATM-106	62	vapor	5.2	S6V - 62	NR	9	--	--	S6V62.dat	1381/172,173	
ATM-106	69	high drip	5.8	S62J - 69	--	--	--	--	--	--	
ATM-106	69	vapor	5.8	S6V - 69	--	--	--	--	--	--	
ATM-106	75	high drip	6.3	S62J -75	--	--	--	--	--	--	
ATM-106	88	high drip	7.3	S62J - 88	NR	3.395	--	--	Finn0600.sz2	1644/68	
ATM-106	92	high drip	7.7	S62J -92	NR	13	--	--	Finn1000.sz2	1644/115-116	
ATM-106	92	high drip	7.7	S62J -92	NR	14.72	--	--	Finn1000.sz2	1644/115-116	
ATM-106	98	high drip	8.2	S62J -98	NR	4.135	--	--	PF041801.sz2	1644/164	
ATM-106	98	high drip	8.2	S62J -98	NR	3.416	--	--	PF041801.sz2	1644/164	

NR size distribution is not resolvable
-- not available or not analyzed
a Average colloid size determined by DLS
b Count rate determined using laser power of 3 mW (514.5 nm argon ion laser)
c Concentration calculated from count rate (at 3 mW) using equation for PS size standard indicated in Size Std Equation column.
d Equation for size standard that is closest in size to the spent fuel colloids (thus only for colloid sizes resolved by DLS).

Appendix 1

Table A1-4. Summary of DLS Analyses on Leachates from ATM-109A, B and C Spent Fuel Corrosion Tests

Waste Form	Gadolinium (%)	Test Duration (months)	Test Type	Test Duration (yr)	Sample ID	Summary of DLS Analyses			Data Reference		Comments
						Size[a] (nm)	Count Rate[b] (kcls)	Conc[c] (particles/L)	DLS Reference	SNI page	
ATM-109A	no	6	high drip	0.5	S9AJ-6	NR	12.1	--	1644/186	PF071701.sz2	
ATM-109A	no	6	high drip	0.5	S9AJ-6	NR	9.159	--	1644/186	PF071701.sz2	
ATM-109C	2%	6	high drip	0.5	S9CJ-6	NR	20	--	1644/186	PF071701.sz2	
ATM-109C	2%	6	high drip	0.5	S9CJ-6	NR	20.4	--	1644/186	PF071701.sz2	
ATM-109A	no	6	vapor	0.5	S9AV-6	NR	0.688	--	1644/186	PF071701.sz2	
ATM-109A	no	6	vapor	0.5	S9AV-6	NR	5.524	--	1644/186	PF071701.sz2	
ATM-109B	no	6	vapor	0.5	S9BV-6	NR	9.114	--	1644/186	PF071701.sz2	
ATM-109B	no	6	vapor	0.5	S9BV-6	NR	8.62	--	1644/186	PF071701.sz2	
ATM-109A	no	12	high drip	1.0	S9AJ-12	--	--	--	--	--	
ATM-109C	2%	12	high drip	1.0	S9CJ-12	--	--	--	--	--	
ATM-109A	no	12	vapor	1.0	S9AV-12	--	--	--	--	--	
ATM-109B	no	12	vapor	1.0	S9BV-12	--	--	--	--	--	
ATM-109A	no	18	high drip	1.5	S9AJ-18	NR	0.782	--	1644/63-64	Finn0600.sz2	
ATM-109C	2%	18	high drip	1.5	S9CJ-18	NR	1.014	--	1644/63-64	Finn0600.sz2	
ATM-109A	no	23	high drip	1.9	S9AJ-23	NR	3.88	--	1644/115-116	Finn1000.sz2	
ATM-109A	no	23	high drip	1.9	S9AJ-23	NR	4.41	--	1644/115-116	Finn1000.sz2	
ATM-109C	2%	23	high drip	1.9	S9CJ-23	NR	4.99	--	1644/115-116	Finn1000.sz2	
ATM-109C	2%	23	high drip	1.9	S9CJ-23	NR	5.09	--	1644/115-116	Finn1000.sz2	
ATM-109A	no	29	high drip	2.4	S9AJ-29	NR	5.682	--	1644/164	PF041801.sz2	
ATM-109A	no	29	high drip	2.4	S9AJ-29	NR	5.252	--	1644/164	PF041801.sz2	
ATM-109C	2%	29	high drip	2.4	S9CJ-29	NR	3.089	--	1644/164	PF041801.sz2	
ATM-109C	2%	29	high drip	2.4	S9CJ-29	NR	3.123	--	1644/164	PF041801.sz2	

NR size distribution is not resolvable

-- not available or not analyzed

a Average colloid size determined by DLS

b Count rate determined using laser power of 3 mW (514.5 nm argon ion laser)

c Concentration calculated from count rate (at 3 mW) using equation for PS size standard indicated in Size Std Equation column.

d Equation for size standard that is closest in size to the spent fuel colloids (thus only for colloid sizes resolved by DLS).

Appendix 2

Data tables for the concentration of Pu-239 and U-238 in leachates and filtrates of CSNF unsaturated tests (reported in units of moles/liter) for test intervals of 5.2 to 8.7 years (ATM-103 and -106 fuels) and 0.5 to 3 years (ATM-109 fuels). Concentrations in unfiltered leachates (UFL) and filtrates from various filters (1000, 450, 200, 50, and 5 nm) were analyzed by alpha spectrometry and ICP-MS and are reported in the following tables.

Table A2-1. Pu-239 Concentrations in ATM-103 HDR Tests

Fuel	Duration	Test Vol	Test	Pu-239 Concentration (in mol/L)						
(Test ID)	(years)	(mL)	pH	UFL (a)	UFL (i)	1000 (i)	450 (a)	200 (a)	50 (a)	5 (a)
ATM-103	5.2	13.55	5.7	bd	bd	–	–	–	–	bd
HDR	5.7	38.75	9.0	4.18E-11	bd	bd	–	–	–	bd
(S32J)	6.3	22.00	6.0	1.74E-11	bd	bd	–	–	9.50E-12	bd
	6.8	0	dry	–	–	–	–	–	–	–
	7.3	29.86	9.0	6.80E-10	bd	bd	4.60E-11	5.53E-11	–	8.07E-11
	7.7	23.96	9.1	5.67E-11	5.83E-09	bd	1.65E-11	6.32E-11	–	–
	8.2	36.7	8.3	–	1.41E-10	5.95E-11	–	–	–	–
	8.7	37.38	8.7	–	3.04E-10	1.57E-10	–	–	–	–

(a) alpha spectrometry data; (i) ICP-MS data

Table A2-2. Pu-239 Concentrations in ATM-103 LDR Tests

Fuel	Duration	Test	Test Vol	Pu-239 Concentration (in mol/L)		
(Test ID)	(years)	pH	(mL)	UFL (a)	UFL (i)	5 (a)
ATM-103	5.2	6.9	5.56	4.43E-09	1.31E-09	2.19E-10
LDR	5.7	7.2	6.88	3.48E-12	bd	–
(S31J)	7.3	dry	0.00	–	–	–

(a) alpha spectrometry data; (i) ICP-MS data

* shaded cells indicate that fuel was found in leachate

Table A2-3. Pu-239 Concentrations in ATM-103 HA Tests

Fuel	Duration	Test	Test Vol	Pu-239 Concentration (in mol/L)		
(Test ID)	(years)	pH	(mL)	UFL (a)	UFL(i)	5 (a)
ATM-103	5.2	6.6	9.14	1.04E-08	7.59E-09	1.95E-09
HA	5.7	nd	2.02	–	5.31E-06	–
(S3V)	7.3	dry	0.00	–	–	–

(a) alpha spectrometry data; (i) ICP-MS data

* shaded cells indicate that fuel was found in leachate

Appendix 2

Table A2-4. Pu-239 Concentrations in ATM-106 HDR Tests

Fuel (Test ID)	Duration (years)	Test pH	Test Vol (mL)	Pu-239 Concentration (in mol/L) UFL (a)	UFL(i)	450 (a)	200 (a)	5 (a)
ATM-106	5.2	6.8	11.85	5.23E-11	9.00E-11	--	--	3.06E-11
HDR	5.7	7.9	38.00	4.21E-12	1.60E-09	--	--	1.97E-12
(S62J)	6.3	6	29.09	5.88E-11	bd	--	--	--
	6.8	9.1	4.47	1.18E-10	bd	2.57E-11	2.37E-11	1.48E-11
	7.3	7.6	21.61	1.44E-10	bd	1.59E-10	4.70E-10	3.67E-11
	7.7	8.6	28.33	2.20E-10	bd	3.17E-11	3.38E-11	--

(a) alpha spectrometry data; (i) ICP-MS data

* shaded cells indicate that fuel was found in leachate

Table A2-5. Pu-239 Concentrations in ATM-106 LDR Tests

Fuel (Test ID)	Duration (years)	Test pH	Test Vol (mL)	Pu-239 Concentration (in mol/L) UFL (a)	UFL(i)	5 (a)
ATM-106	5.2	dry	0	--	--	--
LDR	5.7	6.8	2.24	--	5.13E-07	5.12E-11
(S61J)	7.3	nd	0.27	2.02E-10	1.30E-08	--

(a) alpha spectrometry data; (i) ICP-MS data

* shaded cells indicate that fuel was found in leachate

Table A2-6. Pu-239 Concentrations in ATM-106 HA Tests

Fuel (Test ID)	Duration (years)	Test pH	Test Vol (mL)	Pu-239 Concentration (in mol/L) UFL (a)	UFL(i)	5 (a)
ATM-106	5.2	8.1	10.1	5.59E-08	1.17E-07	8.25E-10
HA	5.7	6.4	8.39	3.16E-12	9.77E-10	--
(S6V)	7.3	dry	0	--	--	--

(a) alpha spectrometry data; (i) ICP-MS data

* shaded cells indicate that fuel was found in leachate

Appendix 2

Table A2-7. Pu-239 Concentrations in ATM-109A HDR Tests

Fuel (Test ID)	Duration (years)	Test pH	Test Vol (mL)	Pu-239 Concentration (in mol/L) UFL (a)	UFL(i)	450 (a)	200 (a)	5 (a)
ATM-109A	0.4	5.7	38.41	1.87E-09	bd	--	--	--
HDR	1	5.5	19.02	2.38E-12	bd	--	--	5.13E-12
(S9AJ)	1.5	7.2	34.87	1.04E-10	bd	3.26E-11	2.93E-11	1.63E-11
	2	8.7	24.19	bd	bd	5.06E-12	bd	bd

(a) alpha spectrometry data; (i) ICP-MS data

Table A2-8. Pu-239 Concentrations in ATM-109A HA Tests

Fuel (Test ID)	Duration (years)	Test pH	Test Vol (mL)	Pu-239 Concentration (in mol/L) UFL (a)	UFL(i)
ATM-109A	0.4	6	9.52	7.16E-10	2.23E-09
HA	1	6.1	9.27	bd	bd
(S9AV)	1.5	dry	0.02	--	--

(a) alpha spectrometry data; (i) ICP-MS data

Table A2-9. Pu-239 Concentrations in ATM-109B HA Tests

Fuel (Test ID)	Duration (years)	Test pH	Test Vol (mL)	Pu-239 Concentration (in mol/L) UFL (a)	UFL(i)
ATM-109B	0.4	5	9.23	5.24E-10	bd
HA	1	7.3	9.85	3.15E-11	bd
(S9BV)	1.5	--	0.05	--	--
	3	dry	--	--	--

(a) alpha spectrometry data; (i) ICP-MS data

Table A2-10. Pu-239 Concentrations in ATM-109C HDR Tests

Fuel (Test ID)	Duration (years)	Test pH	Test Vol (mL)	Pu-239 Concentration (in mol/L) UFL (a)	UFL(i)	450 (a)	200 (a)	5 (a)
ATM-109C	0.4	6.2	36.70	1.36E-09	bd	--	--	--
HDR	1	7.9	29.93	bd	bd	--	--	--
(S9CJ)	1.5	7.8	14.20	4.72E-10	1.49E-09	4.64E-12	7.09E-12	1.12E-11
	2	8.8	19.18	--	bd	--	--	--

(a) alpha spectrometry data; (i) ICP-MS data

Table A2-11. Pu-239 Concentrations in ATM-109C HA Tests

Fuel (Test ID)	Duration (years)	Test pH	Test Vol (mL)	Pu-239 Concentration (in mol/L) UFL (a)	UFL(i)
ATM-109C	0.4	6.7	9.80	1.09E-09	bd
HA	1	6.4	0.72	--	bd
(S9CV)	1.5	--	0.03	--	--

(a) alpha spectrometry data; (i) ICP-MS data

Appendix 2

Table A2-12. U-238 Concentrations in ATM-103 HDR Tests

Fuel	Duration	U-238 Concentrations (in mol/L)							
(Test ID)	(yr)	UFL	Strip	1000 nm	100 nm	50 nm	450 nm	200 nm	5 nm
ATM-103	5.2	2.18E-09	3.38E-07	–	–	–	–	–	–
HDR	5.7	2.27E-07	5.38E-07	1.66E-07	1.58E-07	1.54E-07	–	–	–
(S32J)	6.3	1.59E-09	1.89E-06	4.45E-10	3.74E-10	bd	–	–	–
	6.8	–	1.59E-06	–	–	–	–	–	–
	7.3	5.09E-07	2.93E-06	3.90E-07	1.42E-07	1.38E-07	–	–	–
	7.7	1.98E-06	3.63E-05	3.89E-07	9.20E-08	9.05E-08	–	–	–
	8.2	4.57E-07	1.67E-05	7.51E-08	6.47E-08	6.01E-08	6.14E-08	5.79E-08	5.43E-08
	8.7	5.98E-07	1.82E-05	1.24E-07	8.08E-08	8.08E-08	1.05E-07	7.69E-08	7.52E-08

Note: ICP-MS analyses for U-238 data.

Table A2-13. U-238 Concentrations in ATM-106 HDR Tests

Fuel	Duration	U-238 Concentrations (in mol/L)							
(Test ID)	(yr)	UFL	Strip	1000 nm	100 nm	50 nm	450 nm	200 nm	5 nm
ATM-106	5.2	1.39E-06	3.24E-06	–	–	–	–	–	–
HDR	5.7	3.36E-07	4.64E-06	–	–	–	–	–	–
(S62J)	6.3	9.24E-09	7.68E-07	5.27E-09	5.36E-09	2.91E-09	–	–	–
	6.8	2.88E-08	6.08E-06	–	–	–	–	–	–
	7.3	2.83E-07	1.16E-05	2.94E-07	2.48E-07	9.28E-08	–	–	–
	7.7	7.18E-07	1.02E-04	9.59E-07	7.46E-08	7.94E-08	–	–	–
	8.2	2.73E-07	4.20E-05	4.99E-08	5.95E-08	4.50E-08	8.96E-08	5.40E-08	1.33E-07
	8.7	2.89E-07	1.62E-05	2.49E-07	2.11E-07	1.94E-07	1.68E-07	6.66E-08	2.14E-07

Note: ICP-MS analyses for U-238 data.

Appendix 3

Table A3-1. Summary of dynamic light scattering analyses on colloidal suspension of meta-schoepite and uranium dioxide in 10 mM uranyl nitrate (pH = 5.06).

Sample ID	time elapsed from prep (d)	d1 Size[a] (nm)	d2 Size[a] (nm)	Avg d1 size (nm)	d1 Std Dev (nm)	Count Rate[b] (kc/s)	Conc[c] (coll/L)	Avg Conc (coll/L)	Std Dev Conc (coll/L)	Poly-dispersity	Avg Poly	Std Dev Poly	Conc[c] (ug/mL)	Avg Conc (ug/mL)	Std Dev Conc (ug/mL)
CM1831/10-1	Initial sample prep date = 4/29/2002	--	--	--	--	--	--	--	--	--	--	--	--	--	--
CM1831/10-1	1	193.5	>1000	216	23	152	6.08E+12	5.79E+12	1.25E+12	0.241	0.204	0.035	3.62	3.44E+00	7.44E-01
CM1831/10-1	1	239	>1000			149	5.96E+12			0.186			3.55		
CM1831/10-1	1	214.6	>1000			113.6	4.54E+12			0.161			2.70		
CM1831/10-1	1	199.5	>1000							0.195					
CM1831/10-1	1	202.2	>1000			191.6	7.66E+12			0.240			4.56		
CM1831/10-1	1	254.7	>1000			156.1	6.24E+12			0.236			3.72		
CM1831/10-1	1	205.1				105.8	4.23E+12			0.167			2.52		
CM1831/10-1	3	199.6	>1000	200		139.5	5.58E+12	5.58E+12		0.314	0.314		3.32	3.32E+00	
CM1831/10-1	8	225.3	>1000	205	18	147.1	5.88E+12			0.856			3.50		
CM1831/10-1	8	199.7	>1000			132.3	5.29E+12			0.139			3.15		
CM1831/10-1	8	191.1	>1000			124.1	4.96E+12			0.197			2.95		
CM1831/10-1	17	270.3	>1000	230	58	128.8	5.15E+12	5.22E+12	9.33E+10	0.139	0.188	0.069	3.07	3.10E+00	5.55E-02
CM1831/10-1	17	188.7	>1000			132.1	5.28E+12			0.237			3.14		
CM1831/10-1	30			191	9	133.6	5.34E+12	5.20E+12	1.98E+11		0.354	0.237	3.18	3.10E+00	1.18E-01
CM1831/10-1	30	180.5	>1000			126.6	5.06E+12			0.776			3.01		
CM1831/10-1	30	182.4	>1000							0.292					
CM1831/10-1	30	198.1	>1000							0.221					
CM1831/10-1	30	200.2	>1000							0.245					
CM1831/10-1	30	195.8	>1000							0.237					
CM1831/10-1	70			194	18	84	3.36E+12	3.27E+12	1.22E+11		0.227	0.085	2.00	1.95E+00	7.24E-02
CM1831/10-1	70					79.7	3.19E+12						1.90		
CM1831/10-1	70	174.2	>1000							0.352					
CM1831/10-1	70	213.9	>1000							0.176					
CM1831/10-1	70	202.2	>1000							0.171					
CM1831/10-1	70	184.6	>1000							0.207					
CM1831/10-1	101	213.5	>1000	206	7	58.2	2.33E+12	2.42E+12	1.44E+11	0.243	0.204	0.048	1.39	1.44E+00	8.55E-02
CM1831/10-1	101	205.8	>1000			58.8	2.35E+12			0.151			1.40		
CM1831/10-1	101	199.7	>1000			64.7	2.59E+12			0.218			1.54		

a Colloid size determined by DLS; bimodal distribution (d1 = diameter of one population, d2 = diameter of second population, not resolved using DLS since beyond the range)

b Count rate determined using laser power of 3 mW (514.5 nm argon ion laser)

c Concentration calculated from count rate (at 3 mW) using equation for 100 nm NIST PS size standard.